Chemical Engineering Report Series
Kemian laitetekniikan raporttisarja No. 48
Espoo 2005

VAPOR LIQUID EQUILIBRIUM MEASUREMENTS FOR CLEAN FUEL PROCESSES

Younghun Kim

TEKNILLINEN KORKEAKOULU
TEKNISKA HÖGSKOLAN
HELSINKI UNIVERSITY OF TECHNOLOGY
TECHNISCHE UNIVERSITÄT HELSINKI
UNIVERSITE DE TECHNOLOGIE D'HELSINKI

Chemical Engineering Report Series
Kemian laitetekniikan raporttisarja No. 48
Espoo 2005

VAPOR LIQUID EQUILIBRIUM MEASUREMENTS FOR CLEAN FUEL PROCESSES

Younghun Kim

Dissertation for the degree of Doctor of Science in Technology to be presented with due permission for public examination and debate in Auditorium Ke 2 at Helsinki University of Technology (Espoo, Finland) on the 4th of March, 2005, at 12 o'clock.

Helsinki University of Technology
Department of Chemical Technology
Laboratory of Chemical Engineering and Plant Design

Teknillinen korkeakoulu
Kemian tekniikan osasto
Kemian laitetekniikan ja tehdassuunnittelun laboratorio

Distribution:
Helsinki University of Technology
Laboratory of Chemical Engineering and Plant Design
P. O. Box 6100
FIN-02015 HUT
Tel. + 358-9-4511
Fax. +358-9-451 2694
E-mail: ykim@cc.hut.fi

ISBN 951-22-7482-5
ISSN 1236-875X

Otamedia Oy
Espoo 2005

ABSTRACT

This thesis is based on seven publications dealing with the Vapor Liquid Equilibrium (VLE) measurements which are necessary for pure components process. Two VLE measurements sections were comprised in this thesis. Firstly, VLE runs were conducted with a circulation still at both atmospheric pressure and isothermal conditions under low atmospheric pressure. Secondly, the static apparatus has been used in isothermal VLE for six binary pairs of C4 hydrocarbons and 2-propanone in a range from 69.6 kPa to 610.9 kPa. In addition, the VLE modeling was considered to determine the parameters in thermodynamic models.

The selected components are in area of great industrial interest in view of developing gasoline additives to replace MTBE (2-methoxy-2-methylpropane), such as transform old MTBE plants to produce isooctene. Especially ETBE (2-Ethoxy-2-methylpropane) has emerged as an alternative to MTBE, because ETBE can be produced from ethanol made of renewable resources.

The experimental data were correlated using activity coefficient models for the liquid phase and equation of state (EOS) for the vapor phase. These models were also compared with a predictive activity coefficient models. The estimations made with various different predictive coefficient models gave worse description of the measurements than by fitting the data with the Wilson equation. The experimental apparatus and the procedure presented were shown to be reliable, particularly the computer-controlled static apparatus. Moreover, these results seem to be reliable since they passed thermodynamic consistency tests. Most VLE and excess enthalpy measurements in this thesis are for binary systems that have not been measured previously.

PREFACE

The work of this thesis was carried out during the period 2001 to 2004 in the Laboratory of Chemical Engineering and Plant Design at Helsinki University of Technology. Neste Oy is acknowledged for the scholarship and financial support.

I wish to express my deep gratitude to Professor Juhani Aittamaa for constant encouragement and valuable advice over several years of this study. I am very grateful to D.Sc. Kari I. Keskinen for his wise suggestion and proof-reading the thesis. I thank also pre-examiner Professor Juha Kallas and Professor Josef Novák for their significant helping and revision in completing this thesis.

I would like to express my warm thanks to Petri Uusi-Kyyny for his new ideas and contribution for experimental setup as well as the articles and I am indebted for the inspiration and ideas to Juha-Pekka Pokki for the VLE modeling. I also wish to thank Erlin Sapei, Minna Pakkanen, Lasse M. Westerlund, Virpi Tarkiainen, Raimo A. Ketola as co-authors. I am also very grateful Marko Laakkonen for his contribution in a static apparatus, Piia Haimi for her help in a GC analysis and all the staff in the Laboratory.
I thank also Professor Karel Řehák and Professor Jaroslav Matouš in Prague, Czech Republic, for their positive contribution in the articles.

My special thanks are due to emeritus Professor Dongsup Doh, Professor Byeonghun Min, Professor Hyangkeun Song and Pastor Junho Lee in Korea for their encouragement and interest about studying in Finland.

I offer my sincere thanks to my mother, brother, sister and parents-in-law for their constant support, patience and prayer.
The unconditional support of my wife, Yanghee, and smiling eyes of my children, Yoonsik and Kyusik, were truly invaluable during this work.

Finally, I thank God for giving me the opportunity, ability, confidence and perseverance to write this thesis in Finland.

Espoo, December 2004

Kim, Younghun

LIST OF PUBLICATIONS

This thesis is based on the following publications:

I. Uusi-Kyyny, P.; Tarkiainen, V.; Kim, Y.; Ketola, R. A. and Aittamaa, J., Vapor-Liquid Equilibria for Ethanol + 2,4,4-Trimethyl-1-pentene 2-Propanol + 2,4,4-Trimethyl-1-pentene at 101 kPa, *J. Chem. Eng. Data*, **48** (2003), 280-285.

II. Pokki, J.-P.; Řehák, K.; Kim, Y.; Matouš, J. and Aittamaa, J., Vapor–Liquid Equilibrium Data at 343 K and Excess Molar Enthalpy Data at 298 K for the Binary Systems of Ethanol + 2,4,4-Trimethyl-1-pentene and 2-Propanol + 2,4,4-Trimethyl-1-pentene, *J. Chem. Eng. Data*, **48** (2003), 75-80.

III. Kim, Y.; Pokki, J.-P.; Řehák, K.; Matouš, J. and Aittamaa, J., Excess Enthalpy and Vapor-Liquid Equilibrium at Atmospheric Pressure for Binary Systems for 2-Methyl-2-propanol + 2,4,4-Trimethyl-1-pentene and 2-Butanol + 2,4,4-Trimethyl-1-pentene, *J. Chem. Eng. Data*, **49** (2004), 246-250.

IV. Kim, Y.; Keskinen, K. I. and Aittamaa, J., Vapor-Liquid Equilibrium for Binary Systems of 2-propanol + 2-Ethoxy-2-methylpropane and Ethyl Ethanoate + 2-Ethoxy-2-methylpropane at 333 K and 2-Propanone + 2-Ethoxy-2-methylpropane at 323 K, *J. Chem. Eng. Data*, **49** (2004), 1273-1278.

V. Kim, Y.; Uusi-Kyyny, P.; Pokki, J.-P.; Pakkanen, M.; Multala. R.; Westerlund, L. M. and Aittamaa, J., Isothermal vapor-liquid equilibrium measurements for six binary systems of C4 hydrocarbons + 2-propanone, *Fluid Phase Equilib*., **226** (2004), 173-181.

VI. Uusi-Kyyny, P.; Pokki, J.-P.; Kim, Y. and Aittamaa, J., Isobaric Vapor Liquid Equilibrium for 2,3-Dimethyl-2-butene + Methanol, + Ethanol, + 2-Propanol, or + 2-Butanol at Atmospheric Pressure, *J. Chem. Eng. Data*, **49** (2004), 251-255.

VII. Kim, Y.; Sapei, E.; Keskinen, K. I. and Aittamaa, J., Vapor-Liquid Equilibrium for Binary Systems of 2-Propanol + 1,1-Diethoxyethane at 353 K and Ethyl ethanoate + 1,1-Diethoxyethane at 348 K and 2-Propanone + 1,1-Diethoxyethane at 328 K, *J. Chem. Eng. Data*, accepted for publication on 13. 12. 2004. To be published in 2005.

THE AUTHOR'S CONTRIBUTION

Publication I: The first article had the idea to test if it was possible to use mass spectrometry to analyze samples from VLE measurements. The role of the author was to carry out the experiments together with Petri Uusi-Kyyny.

Publication II: The components presented in this article are important in process design to find alternatives to replace MTBE (2-methoxy-2-methylpropane). Both the vapor-liquid equilibrium and the excess enthalpy data were measured. This way the modeling can be made more reliable compared to VLE data only. The data were modeled with Wilson liquid activity coefficient model. The measurements were done in cooperation with Institute of Chemical Technology, Prague. The author measured VLE data except excess enthalpy.

Publication III: The data measured and presented in this article is part of the same effort as in Publication II. This work extends the previous isothermal data on VLE by excess enthalpy and isobaric VLE and thus the new correlation brought better temperature dependence of the activity coefficient. This led to the third publication where the VLE measurement and writing were all carried out by the author. Institute of Chemical Technology, Prague, accomplished excess enthalpy measurements.

Publication IV: This article is part of an effort to find accurate VLE data for 2-Ethoxy-2-methylpropane (ETBE) with some possible impurities. The author not only modified sampling and mixing chamber parts in experimental setup, but also performed all the work required for publication.

Publication V: This article provides VLE data measurements using a total pressure method for 6 binary systems comprising C4 hydrocarbons with 2-propanone. Especially the measurements in this work were computer-controlled. The author carried out the modeling and writing with the experimental assistance of Minna Pakkanen.

Publication VI: The idea behind this article is that VLE data on C6-alkene + alcohol systems are scarce in the literature. The measurements made are used in the modeling of etherification processes. The role of the author was to carry out the experiments together with Petri Uusi-Kyyny.

Publication VII: This article is part of an effort to find accurate VLE data for a process using or producing ethanol. The investigated components are possible ethanol impurities, when ethanol is produced by fermentation followed by distillation and adsorption. The author finally prepared the manuscript for the article with the experimental assistance of Erlin Sapei.

CONTENTS

NOTATION

A_1, A_2	GC peak areas
A	$=a\alpha P/R^2T^2$, derived parameter of the Soave-Redlich-Kwong (SRK) EOS
B	$=bP/RT$, derived parameter of SRK EOS
A_i B_i C_i D_i	Antoine constants
H^E	excess enthalpy
G^E	excess Gibbs energy
a	attraction parameter of the van der Waals, SRK EOS
$a_{0,12}$ $a_{1,12}$ $a_{2,12}$ $a_{0,21}$ $a_{1,21}$ $a_{2,21}$	temperature dependence parameters in Wilson interaction parameters
a_k $a_{k,0}$ $a_{k,1}$ $a_{k,2}$	parameters of the Legendre polynomial
D - J	Herington's criterion
I	Infinite dilution test's criterion
F_1, F_2	response factors
f	fugacity
f_i^L	fugacity of component i of pure liquid
f_i^{sat}	fugacity of component i at saturation pressure
g	G^E/RT
k_{ij}	binary interaction parameter of the SRK EOS
L_k	Legendre polynomial
m	mass of injected liquid, g
M	molecular weight, g·mol^{-1}
$n_{i,k}^L$	moles of component i of point k in the liquid phase
$n_{i,k}^{tot}$	moles of component i in equilibrium cell in point k
$n_{i,k}^V$	moles of component i of point k in the vapor phase
$n_{V,k}$	total number of moles in the vapor phase of point k
n_1, n_2	moles of components injected in equilibrium cell
NC	number of components
NP	number of points
P	pressure
P_i^{sat}	saturation pressure of i component
P_{exp}	experimental pressure of point k
P_{calc}	calculated pressure of point k
P_{leg}	pressure from Legendre polynomial fit
$P_{i,k}^0$	vapor pressure of pure component i at point k
P_k	total pressure at point k
$\lvert\Delta P_{aver}\rvert$	absolute average pressure residuals between measured and calculated pressure
$\lvert\Delta y_{aver}\rvert$	absolute average vapor fraction residuals between measured and calculated vapor mole fraction, point test's criterion
S	entropy
T	temperature, K
T_1°	boiling point of pure component 1, K
T_2°	boiling point of pure component 2, K
$v_{i,k}^L$	liquid molar volume of component i at point k
v_k^L	liquid molar volume at point k
v_k^V	vapor molar volume at point k

V_i	injected liquid volume of component *i*, m^3
V_i^L	molar volume of component *i* in liquid
v_1^L	molar volume of pure component 1 liquid used in the Wilson equation parameters
v_2^L	molar volume of pure component 2 liquid used in the Wilson equation parameters
$x_{i,k}$	mole fraction of component *i* in liquid phase at point *k*
$y_{i,k}$	mole fraction of component *i* in vapor phase at point *k*
z_i	total mole fraction of component *i* in equilibrium cell
$z_{i,k}$	total mole fraction of component *i* in equilibrium cell at point *k*

Greek letters

α	parameter of the SRK EOS
α_{12}, α_{21}	non-randomness constant for binary *ij* interactions in NRTL model
ϕ_i^{sat}	saturated vapor fugacity coefficient of *i* component
$\phi_{i,k}^0$	fugacity coefficient of pure component *i* at point *k* at the system temperature and vapor pressure of pure component *i*
ϕ_i	fugacity coefficient
$\hat{\phi}_i$	partial fugacity coefficient of species *i* in a mixture
$\phi_{i,k}$	fugacity coefficient of component *i* at point *k* at the system temperature and pressure
κ	isothermal compressibility of liquid, Pa^{-1}
Δ	difference
ρ	density of liquid, $mol \cdot m^{-3}$
Λ_{ij}	adjustable parameters in Wilson's equation
λ_{ij}	binary interaction parameter of the Wilson equation, J/mol
γ_i	activity coefficient of component *i*

Superscripts

´	derivative
E	excess property
L	liquid phase
tot	total
V	vapor phase
0	pure component

Subscripts

calc	calculated
exp	experimental
meas	measured
model	modeled
i, j	components of a mixture
k	data point
r	reduced property

1 Introduction

Vapor liquid equilibrium (VLE) data is necessary for modeling separation processes on various stages of design, development and optimization of chemical plants. In principle predictive vapor-liquid equilibrium model, such as UNIFAC [1], modified UNIFAC [2], and ASOG [3] have been developed from the existing measured VLE data. They can be successfully applied in the preliminary stages of process development when sufficient amount and quality of experimental information of a system is not available. However, when the performance of the studied process is sensitive to vapor-liquid equilibrium, the accuracy of the predictive models is seldom adequate. This is encountered for example within azeotropic distillations. Therefore, this thesis consists of studies on reliable VLE data measurements concerned with chemical process design along with experimental setup and procedure.

EPA (U. S. Environmental Protection Agency) attribute marked improvements in air quality to the use of fuels containing MTBE (2-methoxy-2-methylpropane) and other oxygenates. In Los Angeles, which has had the worst air quality in the USA, the use of reformulated gasoline was credited with reducing ground-level ozone by 18 % during the 1996 smog season, compared to weather-adjusting data for the same period in 1994 and 1995 [4]. Therefore, MTBE production has increased continuously during the last decade. It is used as an octane-enhancing component and it enabled the ban of lead in gasoline. It also enhances gasoline burning and this improves air quality in areas where car density is high. However, leaks in gasoline storage have produced smell and contamination of ground water in some areas, particularly in California [5], where MTBE was banned by the end of 2003. The originally planned ban at the end of 2002 was postponed. New initiatives are required for replacement of MTBE. One option is to transform old MTBE plants to produce isooctene. It is made by dimerization of isobutylene in the presence of alcohol and then hydrogenate iso-octene to iso-octane. The formation of azeotropes between iso-octene and alcohol is possible.

The vapor-liquid equilibrium of alcohols and 2,4,4-trimethyl-1-pentene is thus needed. VLE and excess molar enthalpy for the systems alcohols + 2,4,4-trimethyl-1-pentene at both isothermal and atmospheric pressure were measured, and the results were correlated. Furthermore, the knowledge of the formation of azeotropes in C4 hydrocarbons and 2-propanone systems plays a very important role in modeling and simulation of such processes. In this work, isothermal vapor-liquid equilibrium of six binary systems of C4 hydrocarbons + 2-propanone were measured with the static total pressure method.

In fact, the EU has passed a Directive that will ensure that an even greater percentage of their liquid fuels come from biofuels, which will require that 2 % of petroleum contains biofuels in 2005 and the percentage should gradually rise to 5.75 % by the year 2010. 2-Ethoxy-2-methylpropane (ETBE) has emerged as an alternative to MTBE, because ETBE can be derived from ethanol of renewable resources produced from abundant biomass. Furthermore, ETBE, when compared to MTBE, has a higher octane rating and a lower volatility and is less hydrophilic to permeate and pollute groundwater supplies as well as being chemically more similar to hydrocarbons. In this work, isothermal vapor–liquid equilibrium data for binary system of 2-propanol +

2-ethoxy-2-methylpropane and ethyl ethanoate + 2-ethoxy-2-methylpropane at 333 K and 2-propanone + 2-ethoxy-2-methylpropane at 323 K were measured.

Ethanol can be used as such for gasoline or as a raw material for gasoline component production. Ethanol is produced in vast amounts by fermentation. It is commonly separated from the fermentation broth through distillation to nearly azeotropic ethanol + water mixtures, which are processed by azeotropic distillation or by adsorption masses, such as zeolites, to obtain almost pure ethanol. There are small amounts of side-products of fermentation left in ethanol and also some components are formed due to oxidation during processing. One of these trace components is acetaldehyde, which readily reacts with ethanol to form 1,1-diethoxyethane (acetal). Other trace components present in the ethanol are, for example 2-propanol, ethyl ethanoate, and 2-propanone. These trace components can cause problems in processes using ethanol and containing recycles. Our aim was to study the behavior of 1,1-diethoxyethane with some other components mentioned above. Thus, in this work isothermal vapor–liquid equilibrium data for binary system of for 2-propanol + 1,1-diethoxyethane at 353 K and ethyl ethanoate + 1,1-diethoxyethane at 348 K and 2-propanone + 1,1-diethoxyethane at 328 K were measured.

This thesis comprises two VLE measurements sections. Firstly, VLE runs were conducted with a circulation still of the Yerazunis-type [6] at both atmospheric pressure and isothermal conditions under low atmospheric pressure. Secondly, the static apparatus has been used in isothermal VLE for binary mixture of C4 hydrocarbons and 2-propanone in a range from 69.6 kPa to 610.9 kPa.

2 Thermodynamic Principles

2.1 Vapor Pressure

The vapor pressure of the pure substance was calculated with an Antoine-type equation

$$\frac{P^{\text{sat}}}{\text{MPa}} = \exp\left(A_i - \frac{B_i}{\frac{T}{\text{K}} + C_i} \right) \tag{1}$$

The parameters A, B, and C of this equation were optimized from the data measured in our apparatus. The applicable temperature range is not large and in most instances corresponds to a pressure interval of about 0.01 to 2 bars [7], which have rendered the Antoine equation very popular in correlating low-pressure VLE data. The three-parameter Antoine equations are generally incapable of representing a wide range of temperature from the triple point to the vapor-liquid critical point. There are alternate forms of Antoine equation: extended Antoine equation

$$\frac{P^{\text{sat}}}{\text{MPa}} = \exp\left(A_i + \frac{B_i}{\frac{T}{\text{K}} + C_i} + D_i \ln\left(\frac{T}{\text{K}}\right) \right) \tag{2}$$

$$\frac{P^{\text{sat}}}{\text{MPa}} = \exp\left(A_i + \frac{B_i}{\frac{T}{\text{K}}} + C_i \ln\left(\frac{T}{\text{K}}\right) + D_i \left(\frac{T}{\text{K}}\right)^6 \right) \tag{3}$$

The accurate representation of vapor-pressure data over a wide temperature range requires an equation of greater complexity. The Wagner equation is one of the best available; it expresses the reduced vapor pressure as a function of reduced temperature:

$$P_r^{\text{sat}} = \exp\left(\frac{A_i\tau + B_i\tau^{1.5} + C_i\tau^3 + D_i\tau^6}{1-\tau} \right) \tag{4}$$

where $\tau \equiv 1 - T_r$

2.2 The Evaluation of Fugacity

The dimensionless coefficient $\left(\frac{f}{P}\right)$ is called the fugacity coefficient, that is,

$$\phi = \left(\frac{f}{P}\right) \tag{5}$$

For a component *i* in a solution,

$$\hat{\phi}_i = \frac{\hat{f}_i}{y_i P} \tag{6}$$

Equations of state (such as van der Waals, Soave-Redlich-Kwong and Peng-Robinson) with some variations of mixing rules have been applied to calculate fugacity coefficients for mixtures.
The fugacity coefficient of species *i* in two components is obtained from Soave-Redlich-Kwong (SRK) - EOS as follows,

$$\hat{\phi}_i = \frac{B_i}{B}(z-1) - \ln(z-B) + \frac{A}{B}\left[\frac{B_i}{B} - \frac{2}{a\alpha}\sum_j y_j (a\alpha)_{ij}\right]\ln\left(1+\frac{B}{z}\right) \tag{7}$$

where $(a\alpha)_{ij} = (1-k_{ij})\sqrt{(a\alpha)_{ii}(a\alpha)_{jj}}$

To evaluate the fugacity of a pure liquid at a pressure above the saturation pressure (P^{sat}), that is, for a compressed liquid, a two-step procedure is visualized. First, at saturation the liquid fugacity equals the vapor fugacity, which can be determined from a suitable equation of state (EOS) [8]. Thus,

$$f_i^L = f_i^{sat} = \phi_i^{sat} P_i^{sat} \tag{8}$$

since

$$\phi_i^{sat} = \frac{f_i^{sat}}{P_i^{sat}} \tag{9}$$

In the second step, the change in liquid fugacity with increase in pressure above P_i^{sat} (at constant *T*) is determined. This effect is generally small, but becomes important in high-pressure VLE. The fugacity is related to pressure at constant temperature for a pure material:

$$\mathrm{d}G_i = V_i \mathrm{d}P - S_i \mathrm{d}T = RT\mathrm{d}\ln f_i \tag{10}$$

At constant *T*

$$\mathrm{d}\ln f = \frac{V_i^L}{RT}\mathrm{d}P \tag{11}$$

Integration from P_i^{sat} to P gives the desired relationship:

$$f_i^L = f_i^{sat}\exp\left[\frac{1}{RT}\int_{P_i^{sat}}^{P} V_i^L \mathrm{d}P\right] \tag{12}$$

Returning to basic equation for VLE, Equation ($\hat{\phi}_i y_i P = \gamma_i x_i f_i^o$), relating vapor and liquid mole fractions, and substituting for f_i^o ($= f_i^L$), we obtain

$$y_i P \phi_i = \gamma_i x_i P_i^{sat} \phi_i^{sat} \exp\left[\frac{1}{RT}\int_{P_i^{sat}}^{P} V_i^L \mathrm{d}P\right] \tag{13}$$

where y_i is the mole fraction of component *i* in the vapor phase, *P* is the total pressure of the system, ϕ_i is the fugacity coefficient of component *i* in the vapor phase, x_i is mole fraction of the component *i* in the liquid phase, P_i^{sat} is the saturation pressure (vapor pressure) of pure component *i* at the system temperature, ϕ_i^{sat} is the pure component saturated liquid fugacity coefficient at the system temperature, V_i^L is the molar volume of component *i* in liquid phase at the system temperature, *T* is temperature in Kelvin, and *R* is the universal gas constant (8.31441 $J \cdot K^{-1} \cdot mol^{-1}$). This

is the general equation relating liquid and vapor mole fraction to thermodynamic functions.

2.3 Activity Coefficient Models

Liquid activity coefficient models are used to model liquid phase activity coefficients. There are several models based on different concepts, but their general feature is that the capability to predict the vapor-liquid or liquid-liquid equilibrium is based on the use of experimental data to fit the model parameters for each binary pair. The model parameters are sometimes called interaction energies due to the fact that the formulation of the models requires that parameters have the units of energy (for example, kJ/mol). Liquid activity models such as Wilson [9], NRTL [10] or UNIQUAC [11] have a set of parameters for each binary component pair. In Wilson model, there are two interaction parameters for a composition pair. In addition, for each pure component the molar volume must be known. UNIQUAC also has two interaction parameters for each component pair. In NRTL there are, in principle, three parameters for a component pair, but normally the alfa parameter uses the same value for all component pairs. In this work, the parameters of Wilson, NRTL and UNIQUAC activity coefficient model was optimized.

2.4 Wilson Equation

Wilson model [9] is particularly useful for solutions of polar or associating components (for example, alcohols) in nonpolar solvents.
Wilson presented the following expression for the excess Gibbs energy of a binary solution:

$$\frac{G^{\mathrm{E}}}{RT} = -x_1 \ln\left(x_1 + \Lambda_{12} x_2\right) - x_2 \ln\left(x_2 + \Lambda_{21} x_1\right) \tag{14}$$

The activity coefficients derived from this equation are given by

$$\ln\gamma_1 = -\ln\left(x_1 + \Lambda_{12} x_2\right) + x_2 \left[\frac{\Lambda_{12}}{x_1 + \Lambda_{12} x_2} - \frac{\Lambda_{21}}{\Lambda_{21} x_1 + x_2}\right] \tag{15}$$

and

$$\ln\gamma_2 = -\ln\left(x_2 + \Lambda_{21} x_1\right) - x_1 \left[\frac{\Lambda_{12}}{x_1 + \Lambda_{12} x_2} - \frac{\Lambda_{21}}{\Lambda_{21} x_1 + x_2}\right] \tag{16}$$

Wilson's equation has two adjustable parameters, Λ_{12} and Λ_{21} . In Wilson's derivation, these are related to the molar volume of pure liquid, v_1^L and v_2^L and to characteristic energy differences by

$$\Lambda_{12} = \frac{v_2^L}{v_1^L} \exp\left[-\frac{\lambda_{12} - \lambda_{11}}{RT}\right] \qquad \text{and} \qquad \Lambda_{21} = \frac{v_1^L}{v_2^L} \exp\left[-\frac{\lambda_{21} - \lambda_{22}}{RT}\right] \tag{17}$$

As a result, Wilson's equation not only gives an expression for the activity coefficients as a function of composition, but also an estimate of the variation of the

activity coefficients with temperature. This may provide a practical advantage in isobaric calculations where the temperature varies as the composition changes. For accurate work, $(\lambda_{12} - \lambda_{11})$ and $(\lambda_{21} - \lambda_{22})$ should be considered temperature-dependent. The temperature dependence of the parameters is often described by the expression

$$\lambda_{12} - \lambda_{11} = a_{0,12} + a_{1,12}T + a_{2,12}T^2 \tag{18}$$

$$\lambda_{21} - \lambda_{22} = a_{0,21} + a_{1,21}T + a_{2,21}T^2 \tag{19}$$

2.5 Principle of The Group Contribution Methods

The principle of utilizing a group contribution method is that the molecules in the solution are broken down into so-called functional groups. The number of different functional groups is smaller than the number of different molecules. It is assumed that the physico-chemical properties of a molecule can be obtained as a sum of the properties of the groups. This gives us the possibility to describe the properties of a compound using the interactions between the groups. All group contribution methods are approximate, because the effect of one certain group in one molecule is not necessarily exactly the same as the effect of the same group in another molecule. The basic principle of the effect of a group does not depend on properties of the other groups of molecules. In UNIFAC the activity coefficient is divided into two parts. The development is heavily based on the UNIQUAC model. In UNIQUAC the combinational part of the activity coefficient describes the phenomena caused by size differences of the molecules and the residual part represents the energetic interaction. In UNIFAC model the combinatorial part of UNIQUAC is used, and for the residual, a model based on the group contribution has been developed.

2.6 Excess Enthalpy

The excess enthalpy is obtained from direct calorimetric measurements. The excess Gibbs energy cannot be measured directly, but must be calculated from VLE measurements. The thermodynamic identities that interrelate the excess properties may also be used to calculate one excess property from another. The excess enthalpy is computed from the excess Gibbs energy model. The numerical difference should be sufficient and is the easiest to implement.

$$H^{\mathrm{E}} = -RT^2\left(\frac{\partial\left(\frac{G^{\mathrm{E}}}{RT}\right)}{\partial T}\right)_{P,x} = -RT^2\left(\sum_{i=1}^{NC} x_i \frac{\partial(\ln\gamma_i)}{\partial T}\right)_{P,x} \tag{20}$$

This equation allows calculation of the effect of temperature on the activity coefficient.

2.7 Legendre Polynomials

The activity coefficient model used in the data reduction of the binary pair is Legendre polynomial. The Legendre polynomial is very flexible compared to the local composition models (Wilson, NRTL and UNIQUAC), but the Legendre polynomials should not be used for predictive purposes.
By defining $g = G^E/RT$ the following Legendre polynomial [12] is used

$$g = x_1(1-x_1)\sum_{k=0}^{n} a_k L_k \tag{21}$$

where

$$L_0 = 1 \tag{22}$$

$$L_1 = (2x_1 - 1) \tag{23}$$

$$L_2 = \frac{1}{2}\left[3(2x_1-1)L_1 - 1\right] \tag{24}$$

So, if k is equal or greater than 2

$$L_k = \frac{1}{k}\left[(2k-1)(2x_1-1)L_{k-1} - (k-1)L_{k-2}\right] \tag{25}$$

The derivative of Legendre polynomial with respect to mole fraction x_1 is

$$g' = \frac{\mathrm{d}g}{\mathrm{d}x_1} = (1-2x_1)\sum_{k=0}^{n} a_k L_k + \frac{\mathrm{d}}{\mathrm{d}x_1}\left(\sum_{k=0}^{n} a_k L_k\right)x_1(1-x_1) \tag{26}$$

where

$$\frac{\mathrm{d}L_0}{\mathrm{d}x_1} = 0 \tag{27}$$

$$\frac{\mathrm{d}L_1}{\mathrm{d}x_1} = 2 \tag{28}$$

$$\frac{\mathrm{d}L_2}{\mathrm{d}x_1} = \frac{1}{2}\left[3\left(2L_1 + \frac{\mathrm{d}L_1}{\mathrm{d}x_1}(2x_1-1)\right)\right] \tag{29}$$

So, if k is equal or greater than 2

$$\frac{\mathrm{d}L_k}{\mathrm{d}x_1} = \frac{1}{k}\left[(2k-1)\left(2L_k + \frac{\mathrm{d}L_{k-1}}{\mathrm{d}x_1}(2x_1-1)\right) - (k-1)\frac{\mathrm{d}L_{k-2}}{\mathrm{d}x_1}\right] \tag{30}$$

The coefficients in this study are

$$a_k = a_{k,0} + a_{k,1}T + a_{k,2}T^2 \tag{31}$$

If excess enthalpy is computed the parameters $a_{k,1}$ and $a_{k,2}$ must be nonzero and if only VLE is computed the parameter $a_{k,0}$ are sufficient. Finally, with all these above expressions the activity coefficients are computed from

$$\gamma_1 = \exp\left[g + (1-x_1)g'\right] \tag{32}$$

and

$$\gamma_2 = \exp\left(g - x_1 g'\right) \tag{33}$$

3 Thermodynamic Consistency Tests

3.1 Integral Test [13]

The Gibbs-Duhem equation imposes a general coupling among the partial properties of the components in a mixture and is generally the basis of most methods to test their thermodynamic consistency. Its general form is (Van Ness, 1964 [14])

$$\sum x_i \mathrm{d}\ln\gamma_i = -\frac{\Delta V}{RT}\mathrm{d}P + \frac{\Delta H}{RT^2}\mathrm{d}T \tag{34}$$

At constant temperature and pressure equation 34 may be written for a binary system

$$x_1 \frac{\mathrm{d}\ln\gamma_1}{\mathrm{d}x_1} + x_2 \frac{\mathrm{d}\ln\gamma_2}{\mathrm{d}x_1} = 0 \tag{35}$$

Equation 35 is the basis of the so-called point-to-point test for thermodynamic consistency, but it is of little use, since VLE data are normally measured at either constant temperature or constant pressure. In its integrated form it becomes

$$\int_0^1 \ln\frac{\gamma_1}{\gamma_2}\mathrm{d}x_1 = 0 \tag{36}$$

Equation 36 – applicable to the case of only isothermal vapor-liquid equilibrium – means that if we plot $\ln\frac{\gamma_1}{\gamma_2}$ versus x_1, the areas above (A) and below (B) the x-axis must be equal (Figure 1). This is the so-called area of Redlich-Kister test [15], in which it is assumed that the volume and heat effects of mixing are negligible. In most isothermal cases, the volume of mixing can be safely neglected and a thermodynamic consistency test can be performed according to the Redlich-Kister method. This is not the case for isobaric nonisothermal data for which

$$\int_0^1 \ln\frac{\gamma_1}{\gamma_2}\mathrm{d}x_1 = \int_{T_2^\circ}^{T_1^\circ} \frac{\Delta H}{RT^2}\mathrm{d}T = I \tag{37}$$

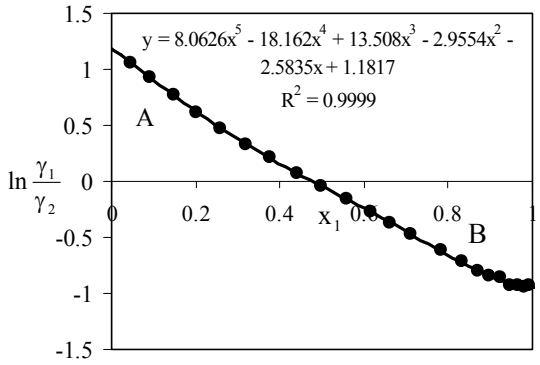

Figure 1. Integral test for the 2-propanol (1) + 2-ethoxy-2-methylpropane (2) at 333 K.

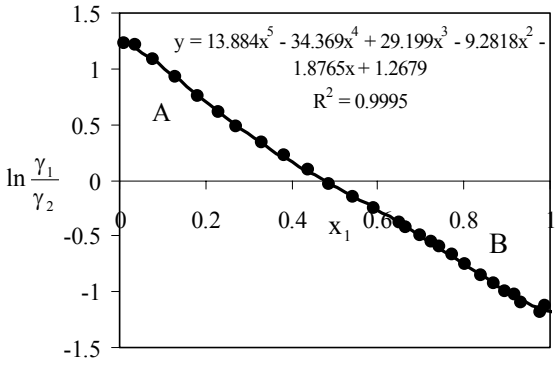

Figure 2. Integral test for the 2-methyl-2-propanol (1) + 2,4,4-Trimethyl-1-pentene (2) at atmospheric pressure.

The right-hand side integral of equation 37 cannot be neglected, and its evaluation requires data on the variation of the heat of mixing with temperature and composition. For consistent data, the value of I represents the difference between areas A and B caused by heat of mixing effects, as well as experimental error. Experimental

information on the variation of heat of mixing with temperature and composition is rarely available, and to overcome this difficulty Herington [16] proposed an empirical test that estimated the value of the right-hand side integral in equation 37 by using as the only parameter the total boiling point range of a mixture. According to Herington, some deviations from the expected behavior will result from small experimental errors, and in the light of experience gained in the application of the test to isothermal data, an uncertainty of 10 units in D may be arbitrarily assigned to this source. Allowance may be made for the effect of these small deviations in the test by postulating that $|D-J|$ must exceed 10 units before the data be considered inconsistent. The Herington criteria then become $|D-J|<10$ for consistent data and $|D-J|>10$ for inconsistent data.

$$D=\frac{100|I|}{\sum}<150\left|\frac{T_{max}-T_{min}}{T_{min}}\right|=J \tag{38}$$

where $\sum$ is the total area A and B of the plot presented in Figure 1 and Figure 2,

In this work, the areas A and B were obtained from integral of $\ln\frac{\gamma_1}{\gamma_2}$ by assistance of solver program in Excel to find an interpolation line.
An example of integral test is shown in Figure 2.

$$D=\frac{100|I|}{\sum}=100\frac{\left|\int_0^1 \ln\frac{\gamma_1}{\gamma_2}dx_1\right|}{|A+B|}=4.0139$$

$$J=150\left|\frac{T_{max}-T_{min}}{T_{min}}\right|=150\left|\frac{374.34-363.73}{363.34}\right|=4.3802$$

$$|D-J|=0.3663$$

3.2 Infinite Dilution Test [17]

It is important to check the consistency of data at the dilute concentration region. Under the conditions of infinite dilutions, the following relationships should be satisfied.

$$\left(\frac{G^{\mathrm{E}}}{RTx_1x_2}\right)_{x_1=0}=\ln\left(\frac{\gamma_1}{\gamma_2}\right)_{x_1=0}=\ln(\gamma_1)_{x_1=0}=\ln\gamma_1^{\infty} \tag{39}$$

$$\left(\frac{G^{\mathrm{E}}}{RTx_1x_2}\right)_{x_2=0}=\ln\left(\frac{\gamma_2}{\gamma_1}\right)_{x_2=0}=\ln(\gamma_2)_{x_2=0}=\ln\gamma_2^{\infty} \tag{40}$$

Infinite dilution test is carried out by the following function based on equation 41 and equation 42,

$$I_1=100\left|I_1^*\right|<30 \tag{41}$$

and

$$I_2 = 100\left|I_2^*\right| < 30 \tag{42}$$

where

$$I_1^* = \left[\frac{\left(\frac{G^E}{RTx_1x_2}\right)_{x_1=0} - \ln\left(\frac{\gamma_1}{\gamma_2}\right)_{x_1=0}}{\ln\left(\frac{\gamma_1}{\gamma_2}\right)_{x_1=0}}\right] \quad \text{and} \quad I_2^* = \left[\frac{\left(\frac{G^E}{RTx_1x_2}\right)_{x_2=0} - \ln\left(\frac{\gamma_2}{\gamma_1}\right)_{x_2=0}}{\ln\left(\frac{\gamma_2}{\gamma_1}\right)_{x_2=0}}\right] \tag{43}$$

As presented in Figures 3 and 4, the infinite dilution test plots show that data measured are not consistent in the dilute region in 2-methyl-2-propanone (1) + 2,4,4-trimethyl-1-pentnene (2) system at atmospheric pressure but good consistent in 2-propanone (1) + 2-ethoxy-2-methylpropane (2) system at 323K.

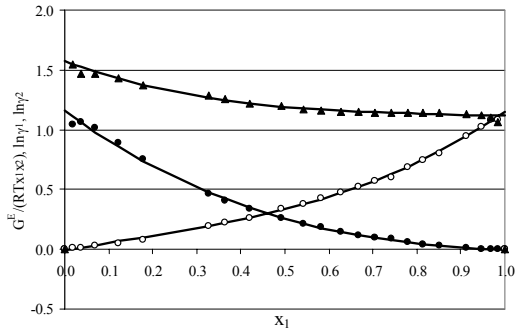

Figure 3. Infinite dilution test for the 2-methyl-2-propanol (1) + 2,4,4-trimethyl-1-pentene (2) system at atmospheric pressure: ▲, $G^E/(TRx_1x_2)$; ●, ln γ_1; ○, ln γ_2 at Original circulation still apparatus.

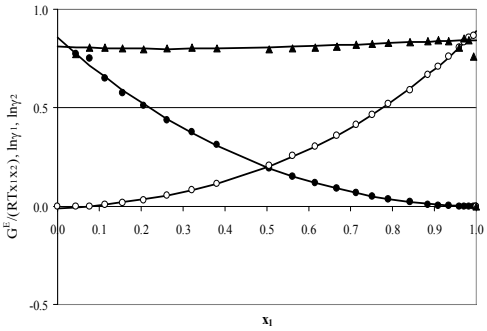

Figure 4. Infinite dilution test for the 2-propanone (1) + 2-ethoxy-2-methylpropane (2) system at 323K: ▲, $G^E/(TRx_1x_2)$; ●, ln γ_1; ○, ln γ_2. at Modified circulation still apparatus.

3.3 Point Test [12]

In the point test, a set of data is considered consistent if the deviation between the model predictions and measured vapor concentrations are smaller than 0.01.

$$\left|\Delta y_{\text{aver}}\right| = \sum_{j=1}^{m} \frac{\left|y_{\text{model}} - y_{\text{meas}}\right|}{m} \tag{44}$$

where m is number of data points

The point test is far more rigorous than the integral test, because each data point is analyzed. It can also serve for finding bad measurements outliers where the deviation between model prediction and actual measurement is exceptionally large and discarding those measurements. As presented in Table 3, all measurements in this study passed successfully this criterion.

4 Experimental Setups and Procedures

4.1 Circulation Still VLE Measurement

4.1.1 Experimental Setup

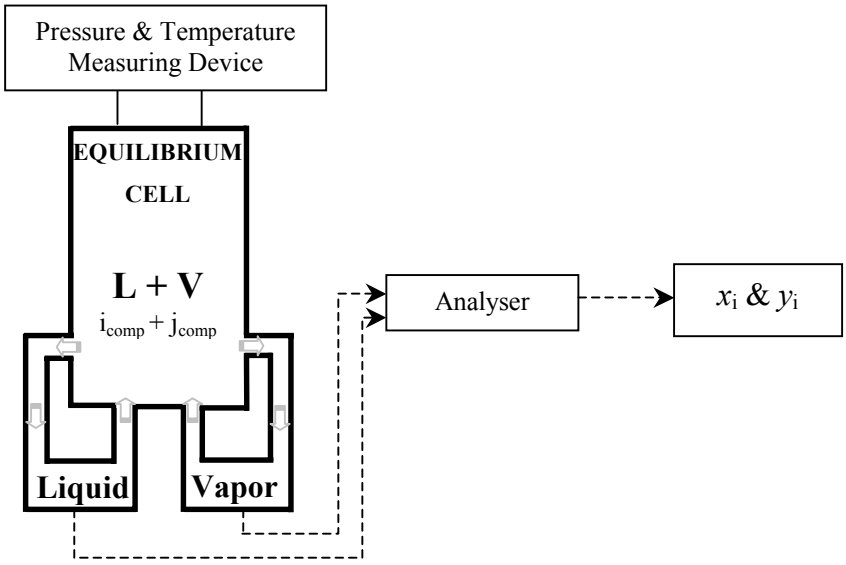

Figure 5. Concept for circulation still apparatus.

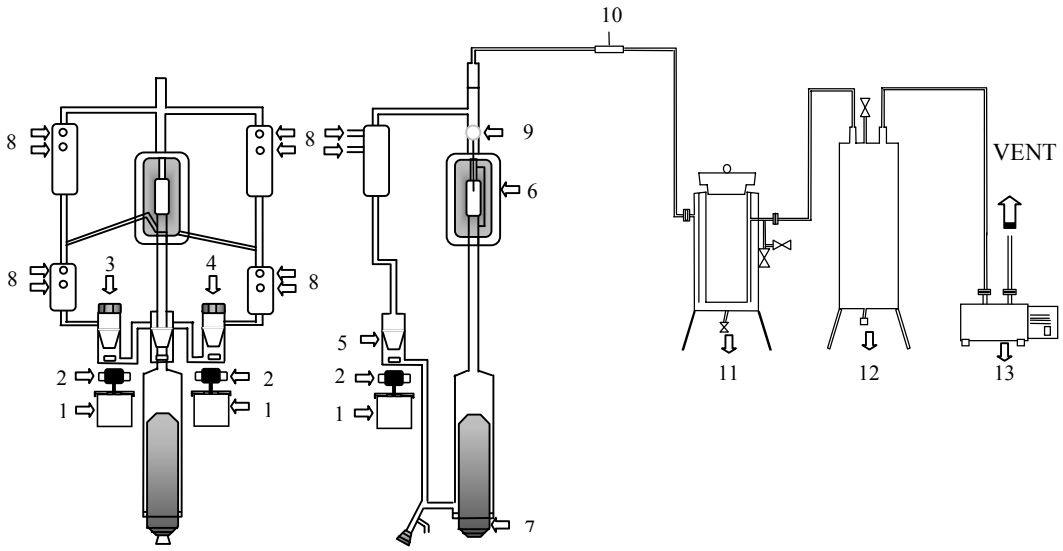

Figure 6. The experimental setup for circulation still apparatus: (1) DC electric motors, (2) Magnetic stirrer bar, (3) Liquid phase chamber, (4) Vapor phase chamber, (5) Mixing chamber, (6) VLE cell, (7) Immersion heater, (8) Cooling water hole, (9) temperature probe (Pt-100), (10) pressure transducer, (11) liquid nitrogen trap, (12) buffer tank 30 dm^3 and (13) vacuum pump.

The VLE runs were conducted with a circulation still of the Yerazunis type [8] built at the glass workshop of Helsinki University of Technology with minor modifications to the original design. Approximately 80 ml of reagents were needed to run the apparatus. The concepts for the circulation still apparatus and for the experimental setup are presented in Figure 5 and Figure 6, respectively. Temperature was measured

with a Thermolyzer S2541 (Frontec) temperature meter with Pt-100 probe calibrated at Inspecta Oy. The Pt-100 probe was located at the bottom of the packed section of the equilibrium chamber. The resolution of the temperature measurement system was 0.005 K and the calibration uncertainty was ±0.015 K. The uncertainty of the whole temperature measurement system is estimated to be ±0.05 K. Pressure was measured with a Druck pressure transducer (0 to 100 kPa) and a Red Lion panel meter. The inaccuracy of the instruments was reported by the manufacturer to be ±0.07 kPa. The pressure measurement system was calibrated against a DHPPC-2 pressure calibrator. The inaccuracy of the whole pressure measurement system including the calibration uncertainty is expected to be less than ±0.15 kPa. In order to improve mixing in the sampling chambers and mixing chamber of the condensed vapor phase and the liquid phase, the DC electric motors were equipped with magnetic stirrer bars, which deliver smooth and consecutive stirring action in chambers.

4.1.2 Analysis of VLE and GC Calibration

The equilibrated liquid phase was cooled and withdrawn from the sample chamber. The equilibrated vapor phase was first condensed and then sampled in liquid phase from the sample chamber. The liquid and vapor samples were analysed with a HP 6850A gas chromatograph with an autosampler and flame ionisation detector (FID). The GC-column used was a HP-1 (methyl siloxane, length 30 - 60 m, nominal diameter 250 – 320 μm, nominal film thickness 0.25 - 1.0 μm). The oven temperature was 100 °C run time 9 - 15 min, inlet split ratio 50:1, carrier gas He (1.0 – 1.4 $mL \cdot min^{-1}$), FID temperature 250 °C. Toluene was used as a solvent for the samples to reduce the volume of the sample.
The response factors were calculated from

$$\frac{A_1}{A_2}\frac{F_1}{F_2} = \frac{x_1}{x_2} \tag{45}$$

where A_1 and A_2 are the GC peak areas, F_1 and F_2 are response factors and x_1 and x_2 are mole fractions of components 1 and 2, respectively. The nine gravimetrically prepared samples per binary system were analyzed and then ratio of A_1/A_2 was plotted as a function of x_1/x_2. The slope of the regressed linear trend is F_2/F_1 and the deviation from origin is called bias. The bias was very small and ignored. Composition of component 1 was solved from

$$x_1 = \frac{A_1F_1}{A_2F_2} \Bigg/ \left(1 + \frac{A_1F_1}{A_2F_2}\right) \tag{46}$$

4.1.3 Procedure

Pure component 1 was introduced to the circulation still and its vapor pressure was measured. Then component 2 was introduced into the equilibrium still. It took approximately 15 to 30 minutes to achieve constant boiling temperature when the differences in boiling point of the pure components were large. The temperature was held constant for approximately 35 minutes to guarantee the steady state condition before sampling. Approximately 1 ml of toluene was added to the 2 ml autosampler vials before sampling was carried out. The samples from the liquid phase and from the vapor condensate were taken with a 1 ml Hamilton Sample Lock syringe. The

syringe was flushed with 0.1 to 0.2 ml of sample before a 0.4 to 0.5 ml sample was taken and injected into the cooled 2 ml autosampler vial.

4.2 Apparatus for Excess Enthalpy Measurements

Excess molar enthalpies were measured with an isothermal microcalorimeter Model 4400 manufactured by Calorimetry Science Corp. (CSC), Provo, USA. This instrument of differential heat conduction design incorporates two test wells (sample and reference) in a large aluminium heat sink that is immersed in an ultra-stable thermostating bath. The microcalorimeter is equipped with flow mixing cells, Model 4442 that have been reconstructed by CSC to improve their performance. Contrary to the original construction using an inefficient mixing tee, in the new design mixing is achieved in a concentric tube arrangement in which the inner tube and the outer tube provide the inlets for two liquids to be mixed.

A schematic diagram of the flow mixing microcalorimeter assembly is presented in Figure 7. Two high-pressure liquid chromatography syringe pumps, Model HPP 5001 by Laboratorní Přístroje (Praha, Czech Republic) were employed to inject the components into the calorimeter. The components are continuously delivered into the sample cell at a constant total flow rate chosen from the range 0.20 to 0.31 ml·min^{-1} while the ratio of individual flow rates is varied to carry out measurements for different compositions. The flow rates can be set with the resolution of 0.01 ml·min^{-1} and the temperature of the fluid in the pump cylinder is measured with a digital thermometer. Calibration of the pump flow rates was done by flowing water through the system while timing and then weighing the delivered amount. Replications showed flow rate reproducibility within 0.3 per cent. The reference cell, which is used to compensate for electronic noise and any heat flux due to temperature fluctuations in the heat sink, is left empty. The differential signal from the calorimeter test wells thus corresponds to the rate of heat production from the sample cell itself. The signal is calibrated using a Joule effect produced by a built-in calibration heater on the pure liquid (before and after each set of experiments). Data acquisition and calibration is controlled by a PC. Details concerning the calorimeter are given elsewhere [18].

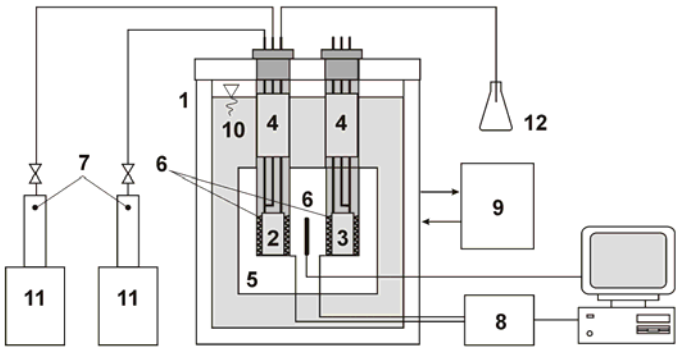

Figure 7. Schematic diagram of the flow mixing microcalorimeter setup: (1) microcalorimeter, (2) sample cell, (3) reference cell, (4) heat exchangers, (5) heat sink, (6) thermoelectric sensors, (7) thermometers, (8) differential amplifier, (9) cooling thermostat, (10) water bath, (11) HPLC syringe pumps and (12) waste bottle.

4.3 Static Total Pressure VLE Measurement

4.3.1 Experimental Setup

Static total pressure apparatus and experimental setup were presented in references [19-21]. The main advantage of the static total pressure method is that no sample withdrawal and analysis is needed. In addition, the time needed for producing one equilibrium point is short. Temperatures of the water bath, syringe pumps, and equilibrium cell were measured with Pt-100 temperature probes connected to the Systemteknik S2541 temperature meter. The temperature meter and probes were calibrated at Finnish National Standards Laboratory. The resolution of the temperature measurement system was 0.005 K and calibration uncertainty was ±0.015 K. The overall uncertainty of the temperature measurement system was estimated to be ±0.03 K. The pressure was measured with a Digiquartz 2100A-101-CE pressure transducer (0-689 kPa) equipped with a Digiquartz 740 intelligent display unit. Calibration of the pressure measurement system was conducted at the Finnish National Standards Laboratory. The uncertainty of the display unit was ±0.069 kPa and the total uncertainty in the pressure measurement system was estimated to be ±0.2 kPa due to limitations in the automation software used. Injections of the components were made with the syringe pumps (Isco 260 D and Isco 100 DM). The temperatures and the pressures of the barrels of the syringe pumps were controlled. The temperatures of the syringe pumps were measured with temperature probes located in contact with the syringe pump barrels.

The equilibrium cell had a total volume of 113.10 cm^3. It was immersed in a 70 dm^3 water bath. The temperature stability of the bath was ±0.02 K. A copper ring was used as a seal between the lid and the cell body. The content of the cell was agitated with a magnetic stirrer. Small baffles were equipped in the equilibrium cell in order to reduce the equilibration time. The valves welded to the lid of the equilibrium cell were operated with Vexta stepping motors. The interface cards connected the stepping motors to the PC. Isco 260 D and Isco 100 DM syringe pumps injected the components to the equilibrium cell and pump volumes were read from Isco control units.

A computer-controlled apparatus, developed from the manually operated version [10], was used. The data transfer between water bath, temperature and pressure meters, stepping motors and syringe pumps, and the PC were operated via a Smartio C168H/8 ports card at a PCI bus. RS232 ports were used for the communication between the PC and the devices. The concept for a static total pressure apparatus and for the experimental setup are presented in Figures 9 and 10.

4.3. 2 Procedure

The targeted injection volumes were optimized so that the equilibrium cell became almost filled with liquid phase at the end of both parts of the measurement. The syringe pumps were operated in constant pressure mode (900 kPa). The Hankinson-Brobst-Thomson-model [22] was used to calculate the compressed liquid density by the compression in the syringe pump. In order to avoid condensation effects on the equilibrium pressure measurement, the pressure transducer and the tube connecting

the pressure transducer to the equilibrium cell were electrically traced and their temperature was adjusted to be higher than the equilibrium cell temperature. The contents of the cell and the bath were mixed continuously during the measurements. Stopping the mixing did not have an effect on the pressure reading after equilibrium was obtained.

In running measurements, the equilibrium point measurements were preceded by pure component vapor pressure measurements. At first, component 1 was introduced into the cell and its vapor pressure was measured. After the vapor pressure measurement of component 1, a predetermined amount of component 2 was added to the equilibrium cell. The cell content was mixed with a magnetic mixer and the cell was allowed to equilibrate for approximately 20 minutes. The readings of the temperature and volume of the pump as well as the pressure and temperature of the equilibrium cell were recorded automatically during all runs. The additions of component 2 were continued until the composition range of approximately 0.5 in mole fraction was reached. The cell was emptied and evacuated and measurements continued with the other side of the isotherm. The cell pressure as a function of total composition should coincide, when the different sides of the isotherm meet at the composition of approximately 0.5 in mole fraction. The measurements are considered to coincide, if the difference between the measured pressures is less than measurement accuracy. If this is not the case, the reason can be leaks in the equilibrium cell or air contamination of the components.

4.3.3 Data Reduction and Error Analysis

The method of Barker [23] was used to calculate composition of vapor phase and liquid phase from total pressure measurements by the VLEFIT-software [24]. Our flow diagram for the data reduction is presented in Figure 11. The method of Barker data reduction assumes that there is a VLE model that can predict the bubble point pressure more accurately than the experimental error of the measured total pressure. The scheme of the data reduction is reported in several publications [23, 25-27]. The data was reduced with Gmehling and Onken polynomial [12] as the activity coefficient model and Soave-Redlich-Kwong [28] cubic equation of state with quadratic mixing rules. Binary interaction parameters k_{ij} in the attraction term of equation of state model were set to the value of zero. All measurements of this work were performed in low pressures where the vapor phase fugacity coefficients are close to one. In those case the effect of interaction parameter is also very small. In high pressures (5 bar) the effect of interaction parameters and vapor phase fugacity coefficients become greater. The uncertainty of injection volumes $\Delta V_1 = \pm 0.02$ cm^3 was obtained from the calibration experiments with distilled water. The estimated inaccuracies of pressure and temperature measurement in the pumps are $\Delta p = \pm 20$ kPa and $\Delta T = \pm 0.1$ K. Densities of the pure components were calculated with a correlation [29]. Uncertainties of density correlation were less than 1.0 % for 1-butene, *n*-butane, and 2-methyl-propane; less than 3.0 % for *cis*-2-butene, 2-methyl-propene, *trans*-2-butene, and 2-propanone. To estimate the uncertainty on overall composition of the mixture in the cell, the theoretical maximum error for an injection is derived below. By differentiating the injected amount of moles n_1 we obtain

$$\mathrm{d}n_1 = \mathrm{d}\left(\frac{\rho_1(T,p)V_1}{M_1} \right) \tag{47}$$

which results as equation for the theoretical maximum error

$$\Delta n_1 = \frac{V_1}{M_1}\Delta\rho_1 + \frac{V_1}{M_1}\left(\left|\frac{\mathrm{d}\rho_1}{\mathrm{d}T}\right|\Delta T + \frac{\mathrm{d}\rho_1}{\mathrm{d}p}\Delta p \right) + \frac{\rho_1}{M_1}\Delta V_1 \tag{48}$$

The modification of the pressure derivative of density gives

$$\Delta n_1 = \frac{V_1}{M_1}\Delta\rho_1 + \frac{V_1}{M_1}\left(\left|\frac{\mathrm{d}\rho_1}{\mathrm{d}T}\right|\Delta T + \left(-\frac{m_1}{V_1^2}\frac{\mathrm{d}V_1}{\mathrm{d}p}\Delta p \right) \right) + \frac{\rho_1}{M_1}\Delta V_1 \tag{49}$$

By taking term $\rho_1 V_1 / M_1 = n_1$ as multiplier

$$\Delta n_1 = n_1\left(\frac{\Delta\rho_1}{\rho_1} + \frac{1}{\rho_1}\left|\frac{\mathrm{d}\rho_1}{\mathrm{d}T}\right|\Delta T + \left(-\frac{1}{V_1}\left(\frac{\mathrm{d}V_1}{\mathrm{d}p}\right)_T \right)\Delta p + \frac{\Delta V_1}{V_1} \right) \tag{50}$$

and setting

$$\kappa_1 = -\frac{1}{V_1}\left(\frac{\mathrm{d}V_1}{\mathrm{d}p}\right)_T \tag{51}$$

which is the isothermal compressibility, we finally obtain

$$\Delta n_1 = n_1\left(\frac{\Delta\rho_1}{\rho_1} + \frac{1}{\rho_1}\left|\frac{\mathrm{d}\rho_1}{\mathrm{d}T}\right|\Delta T + \kappa_1\Delta p + \frac{\Delta V_1}{V_1} \right) \tag{52}$$

Corresponding equation is valid also for the component 2. In equation 52 the temperature derivative of density was calculated from the density correlation [29] and the compressibility of liquid from the Hankinson-Brobst-Thomson-model [22].
Errors in overall mole fractions were determined from

$$\Delta z_1 = \left| \frac{n_1}{n_1 + n_2} - \frac{(n_1 + \Delta n_1)}{(n_1 + \Delta n_1) + (n_2 + \Delta n_2)} \right| \tag{53}$$

The percent relative effect of uncertainty of density, temperature, pressure and injection volume to total uncertainty of injected volume is shown in Figure 8 for *n*-butane + 2-propanone at 330.2 K and it represents typical behavior in measured systems. Effect of uncertainty of density of component *i* increases and of injection volume of component *i* decreases when the mole amount of component *i* increases. Uncertainty of pump temperature and pressure has minor effect on injection uncertainties.

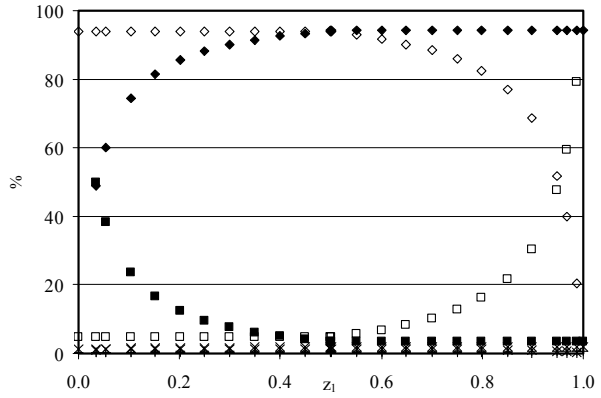

Figure 8. The percent relative effect of uncertainty of density, temperature, pressure and of injection volume to total uncertainty of injected volume for *n*-butane + 2-propanone at 330.2 K. ◆, ◇ Density of n_1 and n_2, respectively, × pump temperature, both n_1 and n_2, + pump pressure, both n_1 and n_2, ■, □ injection volume of n_1 and n_2, respectively.

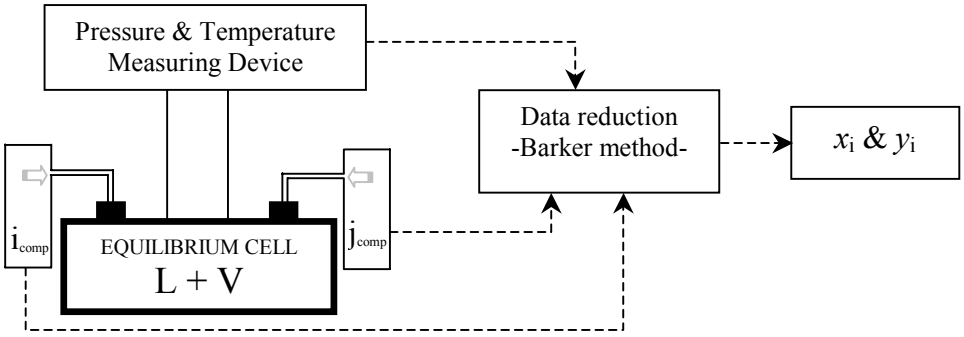

Figure 9. Concept for static total pressure apparatus.

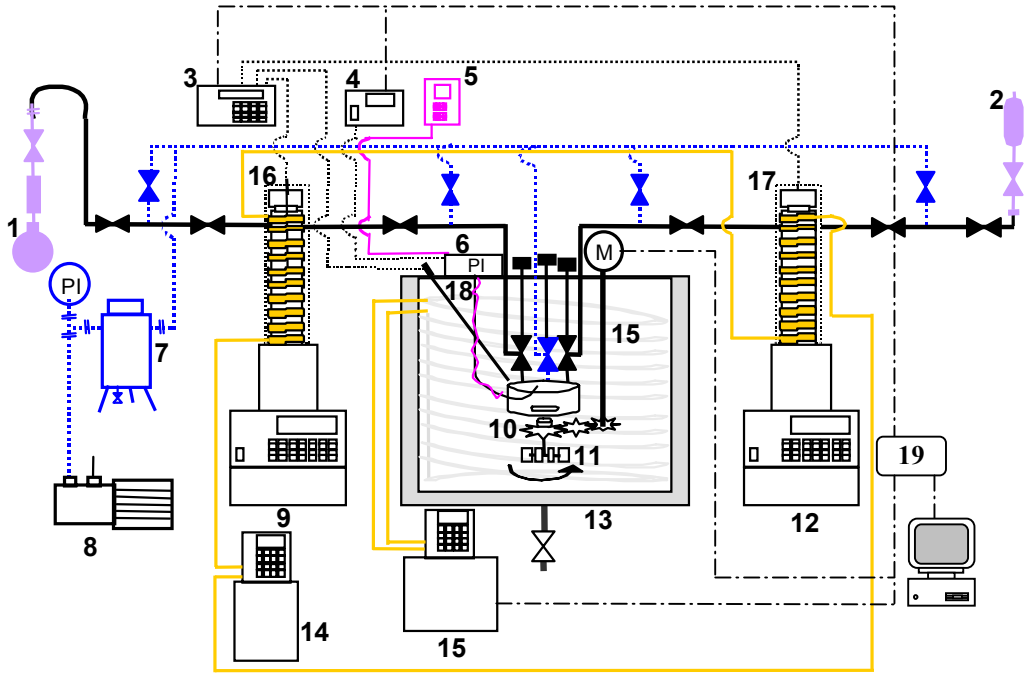

Figure 10. Static total pressure apparatus. (1), (2) feed bottle and cylinder, (3) temperature meter, (4) pressure display, (5) temperature controller for the electric tracing of the pressure transducer and the tube from the equilibrium cell to the pressure transducer, (6) pressure transducer, (7) liquid nitrogen trap, (8) vacuum pump, (9) 260 cm^3 syringe pump, (10) equilibrium cell, (11) bath liquid mixer, (12) 100 cm^3 syringe pump, (13) thermostated water bath, (14) circulator bath for syringe pump temperature control, (15) circulator bath for water bath temperature control, (16), (17), (18) Temperature probes (Pt-100), (19) PCI bus, ▬ feed line to cell and to syringe pump, ▬ water line for the temperature control of the syringe pump and the bath, ····· vacuum line.

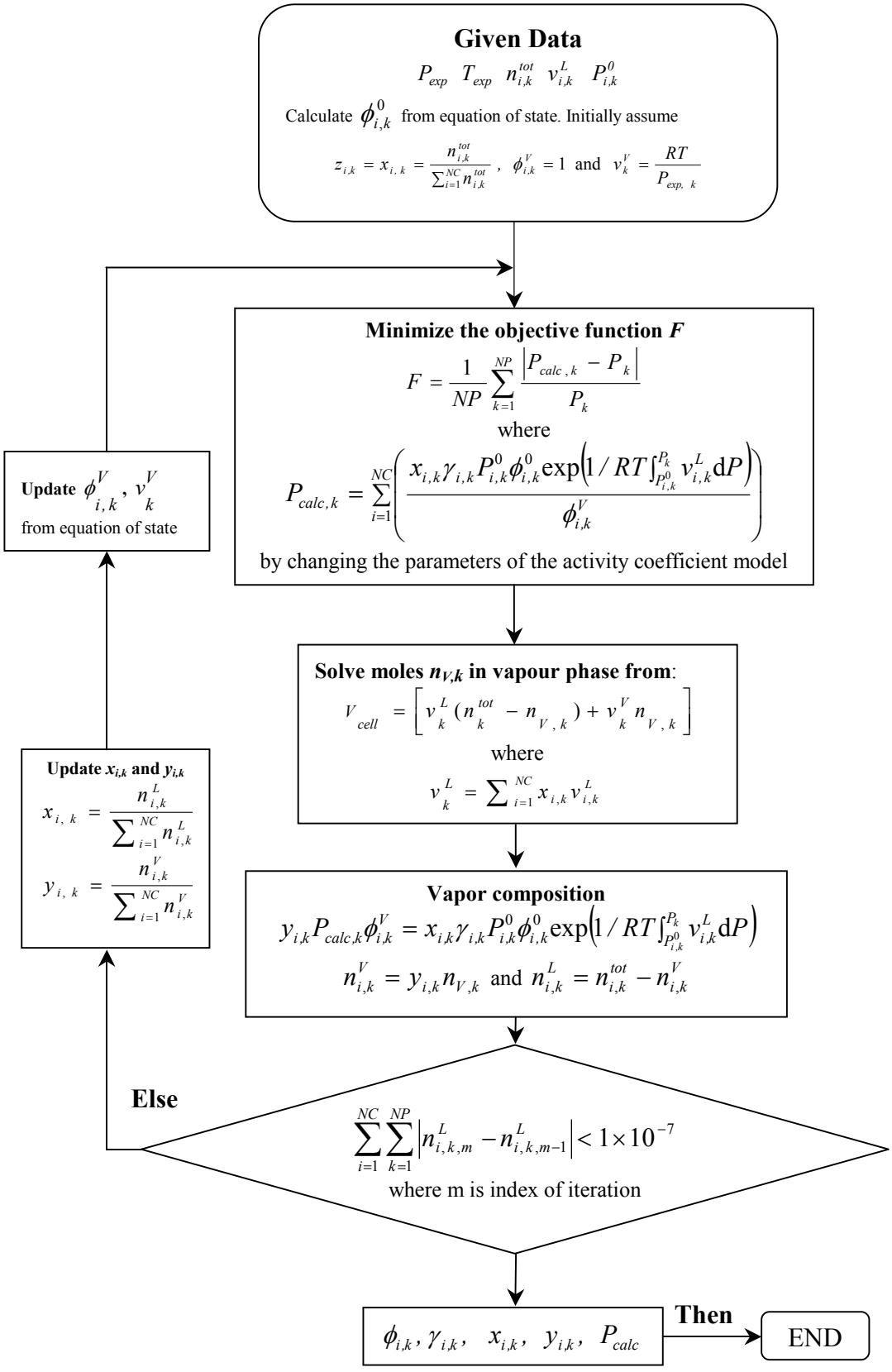

Figure 11. Flow diagram for data reduction.

5 Results and Discussion

This chapter summarizes the results obtained. The first section discusses evaluating the VLE data in the circulation still. The results from static total pressure apparatus are presented in the following section. The chapter closes with a summary table of data reduction results on evaluation of deviation and parameters for the correlation model (Wilson [9], NRTL [10] and UNIQUAC [30]).

5.1 VLE data in the Circulation Still

The experimental conditions for binary VLE systems conducted with a circulation still are presented in Table 1.

Table 1. Experimental conditions at circulation still

Component 2 / Component 1	**2,4,4-Trimethyl-1-pentene**		**2,3-Dimethyl-2-butene**	**1,1-Diethoxyethane**	**2-ethoxy-2-methylpropane**
Experimental setup	Circulation still				
2-Methyl-2-propanol	Atmospheric pressure	Excess Enthalpy at 300 K			
2-Butanol	Atmospheric pressure	Excess Enthalpy at 298 K	Atmospheric pressure		
Ethanol	Atmospheric pressure Isothermal data at 343.43 K	Excess Enthalpy at 298 K	Atmospheric pressure		
2-Propanol	Atmospheric pressure Isothermal data at 343.43 K	Excess Enthalpy at 298 K	Atmospheric pressure	Isothermal data at 353 K	Isothermal data at 333 K
Methanol			Atmospheric pressure		
2-Propanone				Isothermal data at 348 K	Isothermal data at 323 K
Ethyl acetate				Isothermal data at 328 K	Isothermal data at 333 K

All binary systems in this thesis exhibit positive deviations from Raoult's law. Azeotropic behavior was observed as either a maximum or minimum boiling point in the isothermal system or atmospheric system. The azeotropic data were determined graphically from the measured values (*Px* and *Tx* curve). Results of azeotropic point in circulation still are presented in Table 2.
The occurrence of an azeotrope is indicated by an extreme in the equilibrium pressure on a composition-pressure diagram or in the equilibrium temperature on a composition-temperature diagram as shown in Figure 12 and 13 respectively.

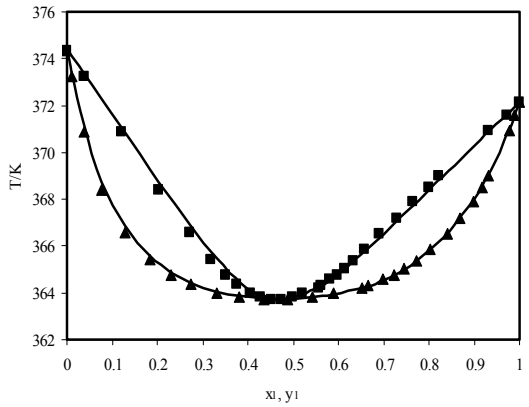

Figure 12. Temperature-composition diagram for the 2-butanol (1) + 2,4,4-trimethyl-1-pentene (2) system at atmospheric pressure: ▲, x_1 from data; ■, y_1 from data; —, x_1, y_1 by the Wilson model data.

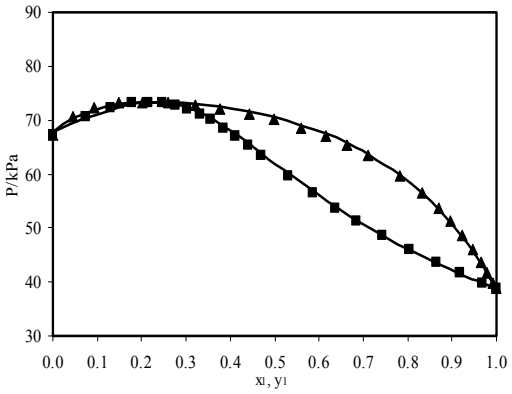

Figure 13. Pressure-composition diagram for the 2-propanol (1) + 2-ethoxy-2-methylpropane (2) system at 333 K: ▲, x_1 from data; ■, y_1 from data; —, x_1, y_1 by the Wilson model data.

Table 2. Results of azeotropic point at circulation still

Binary pair	Azeotropic point		
	P/kPa	T/K	x_{1az}
2-Methyl-2-propanol (1) + 2,4,4-Trimethyl-1-pentene (2)	100.5	352.83	0.73
2-Butanol (1) + 2,4,4-Trimethyl-1-pentene (2)	101.2	363.72	0.46
Ethanol (1) + 2,4,4-Trimethyl-1-pentene (2)	92.1	343.43	0.66
2-Propanol (1) + 2,4,4-Trimethyl-1-pentene (2)	75.5	343.43	0.65
Ethanol (1) + 2,4,4-Trimethyl-1-pentene (2)	101	345	0.676
2-Propanol (1) + 2,4,4-Trimethyl-1-pentene (2)	101	351	0.670
2,3-Dimethyl-2-butene (1)+ Methanol (2)	101.2	325.4	0.468
2,3-Dimethyl-2-butene (1) + Ethanol (2)	100.7	334.8	0.614
2,3-Dimethyl-2-butene (1) + 2-Propanol (2)	100.0	338.7	0.696
2,3-Dimethyl-2-butene (1) + 2-Butanol (2)	101.8	345.1	0.895
2-Propanol (1) + 1,1-Diethoxyethane (2)	73.3	333	0.230
2-Propanone (1) + 1,1-Diethoxyethane (2)	84.35	323	0.821
Ethyl acetate (1) + 1,1-Diethoxyethane (2)	69.20	333	0.271
2-Propanol (1) + 2-Ethoxy-2-methylpropane (2)	94.2	353	0.916

In principle, the composition of the azeotropic mixture can be affected by changing pressure. At a low pressure, the liquid phase may split to two phases due to liquid non-ideality.

The Soave-Redlich-Kwong equation of state with quadratic mixing rules in the attractive parameter and linear in covolume was used to calculate fugacity coefficients. The binary interaction parameters of the SRK equation were set to zero for systems in this study. This is justified by the low pressure, which makes the vapor

phase nearly ideal. To clarify this point, we used the SRK equation of state to take into account the non-ideality in vapour phase. The fugacity coefficients are very close to unity in our systems. They do not vary significantly as a function of binary interaction parameter. The objective function is insensitive to SRK binary interaction parameters. So it was not possible to evaluate the value of the SRK parameter properly. It is believed that the non-ideality is mostly in the liquid phase, not in the vapour phase. Vapour phase nearly ideal is caused most obviously by low system pressure.

During the parameter fitting of the Wilson equation, VLE and VLE+H^E (Excess Enthalpy) measurements were correlated simultaneously. The following objective functions were used by using VLEFIT [24]

$$O.F. = \frac{1}{N_{\mathrm{VLE}}} \sum_{i=1}^{N_{\mathrm{VLE}}} \left(\frac{P_{\mathrm{model}} - P_{\mathrm{meas}}}{P_{\mathrm{meas}}} \right)^2 \qquad \text{Paper VII} \qquad (54)$$

$$O.F. = \frac{1}{N_{\mathrm{VLE}}} \sum_{i=1}^{N_{\mathrm{VLE}}} \frac{\left| P_{\mathrm{model}} - P_{\mathrm{meas}} \right|}{P_{\mathrm{meas}}} \qquad \text{Paper IV} \qquad (55)$$

$$O.F. = \frac{1}{N_{\mathrm{VLE}}} \sum_{i=1}^{N_{\mathrm{VLE}}} \sum_{j=1}^{2} \left(\gamma_{i,j,\mathrm{model}} - \gamma_{i,j,\mathrm{meas}} \right)^2 \qquad \text{Paper I} \qquad (56)$$

$$O.F. = \frac{1}{N_{\mathrm{VLE}}} \sum_{i=1}^{N_{\mathrm{VLE}}} \sum_{j=1}^{2} \left| \frac{\gamma_{i,j,\mathrm{model}} - \gamma_{i,j,\mathrm{meas}}}{\gamma_{i,j,\mathrm{meas}}} \right| \qquad \text{Paper VI} \qquad (57)$$

$$O.F. = \frac{1}{N_{\mathrm{VLE}}} \sum_{i=1}^{N_{\mathrm{VLE}}} \sum_{j=1}^{2} \left| \frac{\gamma_{i,j,\mathrm{model}} - \gamma_{i,j,\mathrm{meas}}}{\gamma_{i,j,\mathrm{meas}}} \right| + \frac{1}{N_{\mathrm{HE}}} \sum_{1}^{N_{\mathrm{HE}}} \left| \frac{H^{\mathrm{E}}_{i,\mathrm{model}} - H^{\mathrm{E}}_{i,\mathrm{meas}}}{H^{E}_{i,\mathrm{meas}}} \right| \qquad \text{Paper III} \qquad (58)$$

$$O.F. = \frac{1}{N_{\mathrm{VLE}}} \sum_{1}^{N_{\mathrm{VLE}}} \frac{\left(P_{i,\mathrm{model}} - P_{i,\mathrm{meas}} \right)}{P_{i,\mathrm{meas}}} + \frac{1}{N_{\mathrm{HE}}} \sum_{1}^{N_{\mathrm{HE}}} \frac{\left(H^{\mathrm{E}}_{i,\mathrm{model}} - H^{\mathrm{E}}_{i,\mathrm{meas}} \right)}{H^{\mathrm{E}}_{i,\mathrm{meas}}} \qquad \text{Paper II} \qquad (59)$$

We chose objective function respectively to optimize model with measured data as shown in above equations.
The liquid phase was modeled with the Wilson equation. The critical temperature, critical pressure, acentric factor and the liquid molar volume for each component are needed in the calculation.
The results of the integral test [13], the infinite dilution test [17], the point test [17], and the parameters of the models are presented in Table 3 - 6.

Slight inconsistency of the correlated data series caused the deviation Δy ($y_{\mathrm{model}} - y_{\mathrm{meas}}$) and ΔT (T_{model} - T_{meas}) to be not randomly scattered about their zero values as shown in Figure 14. One reason for this behavior is believed to lie in the mixing in the sampling chambers and in the mixing chamber of the condensed vapor phase and liquid phase. To improve mixing in the sampling chambers and in the mixing chamber of the condensed vapor phase and the liquid phase, the DC electric motors were equipped with magnetic stirrer bars, which deliver smooth and consecutive stirring action in chambers.

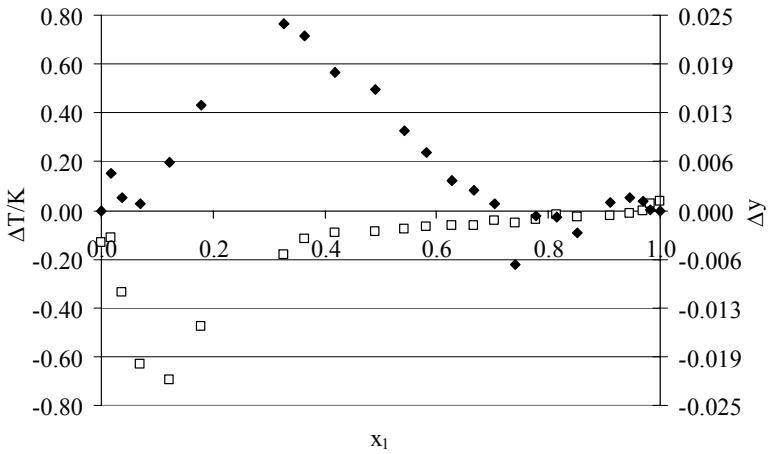

Figure 14. Point test for the 2-methyl-2-propanol (1) + 2,4,4-trimethyl-1-pentene (2) system at atmospheric pressure: ◆; Δ*y*, □; Δ*T*.

In paper IV, VLE measurements of 2-propanol + 2-ethoxy-2-methylpropane and ethyl ethanoate + 2-ethoxy-2-methylpropane were made near the lower limit of measured pure-component vapor pressure of 2-propanol and ethyl ethanoate. The extrapolation of VLE to lower temperature required the extrapolation of the pure component vapor pressure. The extrapolation capability of Antoine parameters optimized in this work was checked against the Antoine parameters reported in the literature. The extrapolation did not show significant difference as presented in Figure 15.

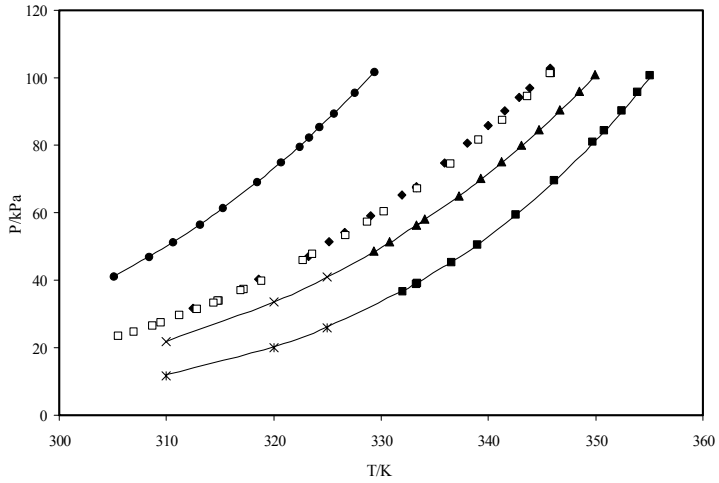

Figure 15. Vapor pressure of pure substances: ◆, 2-ethoxy-2-methylpropane, measured, this work; □, 2-ethoxy-2-methylpropane, Krähenbühl and Gmehling[31]; ■, 2-propanol, measured, this work; ∗ extrapolated data with Antoine parameters optimized in this work; ●, 2-propanone, measured, this work; ▲, ethyl ethanoate, measured, this work; × extrapolated data with Antoine parameters optimized in this work; —, calculated from Antoine constants in the literature.[7]

In this study at circulation still, The VLE data of the binary systems was correlated using local composition models. The parameters of the Wilson, NRTL and UNIQUAC equations were obtained by minimizing the objective function. The Wilson equations gave a good fit if compared to the group contribution method UNIFAC. For the other activity coefficient models, the situation differs from case to case.

Table 3. Results of consistency tests for binary systems in the circulation still

Values of consistency functions					Result of consistency tests				
$\lvert D - J \rvert$	$\lvert D \rvert$	I_1	I_2	$\lvert \Delta y_{aver} \rvert$	$\lvert D - J \rvert$	$\lvert D \rvert$	I_1	I_2	$\lvert \Delta y_{aver} \rvert$
0.5	8.5	36.1	3.0	0.006	+	+	–	+	+
2-Methyl-2-propanol (1) + 2,4,4-Trimethyl-1-pentene (2)					**Atmospheric pressure data**				
0.4	4.4	16.9	-16.2	0.004	+	+	+	+	+
2-Butanol (1) + 2,4,4-Trimethyl-1-pentene(2)					**Atmospheric pressure data**				
	0.02	22.3	29.6	0.004		+	+	+	+
Ethanol (1) + 2,4,4-Trimethyl-1-pentene(2)					**Isothermal data, T = 343.43 K**				
	3.09	17.6	25.6	0.008		+	+	+	+
2-Propanol (1) + 2,4,4-Trimethyl-1-pentene (2)					**Isothermal data. T = 343.43 K**				
		44.7	-14.8	0.0080			–	+	+
Ethanol (1) + 2,4,4-Trimethyl-1-pentene (2)					**Atmospheric pressure data**				
		5.5	13.7	0.0036			+	+	+
2-Propanol (1) + 2,4,4-Trimethyl-1-pentene (2)					**Atmospheric pressure data**				
8.3	1.3			0.0059	+	+			+
2,3-Dimethyl-2-butene (1) + Methanol (2)					**Atmospheric pressure data**				
6.4	1.0			0.0008	+	+			+
2,3-Dimethyl-2-butene (1) + Ethanol (2)					**Atmospheric pressure data**				
7.2	0.2			0.0037	+	+			+
2,3-Dimethyl-2-butene (1)+ 2-Propanol (2)					**Atmospheric pressure data**				
11.3	0.6			0.0052	+	+			+
2,3-Dimethyl-2-butene (1) + 2-Butanol (2)					**Atmospheric pressure data**				

Table 3. Results of consistency tests for binary systems in the circulation still

Values of consistency functions					Result of consistency tests				
$\lvert D - J \rvert$	$\lvert D \rvert$	I_1	I_2	$\lvert \Delta y_{aver} \rvert$	$\lvert D - J \rvert$	$\lvert D \rvert$	I_1	I_2	$\lvert \Delta y_{aver} \rvert$
	2.8	-1.7	-5.9	0.003		+	+	+	+
2-Propanol (1) + 1,1-Diethoxyethane (2)					**Isothermal data, K = 353 K**				
	1.2	-4.3	-13.9	0.003		+	+	+	+
2-Propanone (1) + 1,1-Diethoxyethane (2)					**Isothermal data, K = 328 K**				
	7.5	12.0	6.8	0.001		+	+	+	+
Ethyl acetate (1) + 1,1-Diethoxyethane (2)					**Isothermal data, K = 348 K**				
	1.3	16.1	-8.1	0.002		+	+	+	+
2-Propanol (1) + 2-Ethoxy-2-methylpropane (2)					**Isothermal data, K = 333 K**				
	0.7	-5.1	-4.9	0.002		+	+	+	+
2-Propanone (1) + 2-Ethoxy-2-methylpropane (2)					**Isothermal data, K = 323 K**				
	3.5	-4.6	5.4	0.001		+	+	+	+
Ethyl acetate (1) + 2-Ethoxy-2-methylpropane (2)					**Isothermal data, K = 333 K**				

Table 4. Results of Average of Absolute Vapor Fraction Residuals Δy , Temperature Residuals ΔT/K(Atmospheric pressure system) and Pressure Residuals ΔP/kPa (Isothermal temperature system) for the Wilson Fit, Fitted Wilson interaction parameters for the mixtures: $\lambda_{12}-\lambda_{11} = a_{0,12} + a_{1,12}\times T + a_{2,12}\times T^2$, $\lambda_{21}-\lambda_{22} = a_{0,21} + a_{1,21}\times T + a_{2,21}\times T^2$

Binary pair	$\lvert\Delta y_{aver}\rvert$	Wilson interaction parameter				
	Average Residuals	$a_{0,12}$ $a_{0,21}$	$a_{1,12}$ $a_{1,21}$	$a_{2,12}$ $a_{2,21}$	$\lambda_{12}-\lambda_{11}$	$\lambda_{21}-\lambda_{22}$
Component 1 Component 2	Wilson	$J\cdot mol^{-1}$	$J\cdot mol^{-1}\cdot K^{-1}$	$J\cdot mol^{-1}\cdot K^{-2}$	$J\cdot mol^{-1}$	
2-Methyl-2-propanol	0.006	3849.176	16.66556	-0.0414		
2,4,4-Trimethyl-1-pentene	0.137 $\lvert\Delta T_{aver}\rvert$	-1254.9096	17.24417	-0.04025		
2-Butanol	0.004	5665.996	17.86256	-0.05763		
2,4,4-Trimethyl-1-pentene	0.065 $\lvert\Delta T_{aver}\rvert$	962.9221	0.679811	-0.00765		
Ethanol	0.004	5773.6	22.4412	-0.0488		
2,4,4-Trimethyl-1-pentene	0.41 $\lvert\Delta P_{aver}\rvert$	1071.1	2.4855	-0.009		
2-Propanol	0.008	5718.7	17.8814	-0.0517		
2,4,4-Trimethyl-1-pentene	0.35 $\lvert\Delta P_{aver}\rvert$	842.67	0.66721	-0.0042		
Ethanol	0.008					
2,4,4-Trimethyl-1-pentene	0.39 $\lvert\Delta T_{aver}\rvert$				7043.8	1631.8
2-Propanol	0.0036					
2,4,4-Trimethyl-1-pentene	0.22 $\lvert\Delta T_{aver}\rvert$				5544.2	521.03

Table 5. Results of Average of Absolute Vapor Fraction Residuals Δy, Temperature Residuals ΔT/K for the Wilson, NRTL, UNIQUAC, UNIFAC and UNIFAC-Dortmund Fits, Fitted Wilson and NRTL interaction parameters for the mixtures in Atmospheric pressure system

Binary pair	Atmospheric Pressure System					Wilson Parameters		NRTL Parameter	
	$\lvert\Delta y_{aver}\rvert$ / $\lvert\Delta T_{aver}\rvert/T$					λ_{12}-λ_{11}	λ_{21}-λ_{22}	g_{12}-g_{11}	g_{21}-g_{22}
1 component 2 component	**Wilson**	**NRTL**	**UNIQUAC**	**UNIFAC**	**UNIFAC-Dortmund**	$J \cdot mol^{-1}$		K	
2,3-Dimethyl-2-butene	0.0059	0.0124	0.0194	0.0209	0.0067	2110.7	9488.5	691.87	513.14
Methanol	0.14	0.41	0.28	1.07	0.28				
2,3-Dimethyl-2-butene	0.0008	0.0072	0.0108	0.0069	0.0103	1173.4	7235.4	543.83	378.28
Ethanol	0.14	0.24	0.32	0.18	0.41				
2,3-Dimethyl-2-butene	0.0037	0.0064	0.0081	0.0104	0.0140	771.15	5594.8	497.72	229.40
2-Propanol	0.11	0.19	0.24	0.50	0.66				
2,3-Dimethyl-2-butene	0.0052	0.0055	0.0056	0.0148	0.0115	261.63	4821.6	451.10	117.42
2-Butanol	0.23	0.28	0.31	1.21	0.36				

Table 6. Results of Average of Absolute Vapor Fraction Residuals Δy and Pressure Residuals ΔP/kPa for the Wilson, NRTL and UNIFAC Fits, Fitted Wilson and NRTL interaction parameters for the mixtures in Isothermal temperature system

Binary pair	Isothermal temperature system			Wilson Parameters		NRTL Parameters	
	$\lvert\Delta y_{aver}\rvert$ / $\lvert\Delta P_{av}\rvert$/kPa			λ_{12}-λ_{11}	λ_{21}-λ_{22}	g_{12}-g_{11}	g_{21}-g_{22}
1 component 2 component	Wilson	NRTL	UNIFAC	J·mol^{-1}		K	
2-Propanol	0.003	0.002	0.006				
1,1-Diethoxyethane	0.27	0.29	0.74	2365.518	-9.984	229.84	53.354
2-Propanone	0.003	0.003	0.007				
1,1-Diethoxyethane	0.15	0.14	0.66	3140.713	-1660.002	8.4812	167.07
Ethyl acetate	0.001	0.002	0.007				
1,1-Diethoxyethane	0.23	0.33	0.47	399.301	111.522	28.229	14.082
2-Propanol	0.002						
Ethyl tertiary butyl ether	0.26			3904.3	-352.85		
2-Propanone	0.002						
Ethyl tertiary butyl ether	0.13			2826.9	-368.04		
Ethyl acetate	0.001						
Ethyl tertiary butyl ether	0.03			1093.6	19.13		

5.2 VLE data in Static Total Pressure Apparatus

In paper V, the experimental conditions for binary VLE systems conducted with a static apparatus are presented in Table 7. Total pressure measurements were performed to obtain *PTz* data. The measurements are treated using the Barker's method to provide *PTxy*. VLE data have been correlated by Wilson, UNIQUAC, and NRTL activity coefficient models as well as using Legendre polynomials.

Table 7. Experimental Condition at Static Apparatus

Component 2 / Component 1	**2-propanone**
Experimental setup	Static apparatus
***n*-butane**	Isothermal data at 330.2 K
2-methyl-propane	Isothermal data at 318.6 K
1-butene	Isothermal data at 323.3 K
***cis*-2-butene**	Isothermal data at 331.9 K
2-methyl-propene	Isothermal data at 323.1 K
***trans*-2-butene**	Isothermal data at 332.1 K

All six binary pairs measured show a positive deviation from Raoult's law. Azeotropic point was found for the *n*-butane (1) + 2-propanone (2) pair experimentally and from Legendre polynomial fit at $x_1 = 0.99$, $T = 330.17$ K and $P = 593.0$ kPa. The other measured systems did not show azeotropic behavior as represented in Figure 16. In all six runs, the pressure coincided well when the different sides of the binary met. Parameters of the Legendre polynomial are summarized in Table 8. The pressure residuals from the Legendre polynomial regression are extremely small. When comparing the NRTL, Wilson, and UNIQUAC [30] models which were used in the regressions presented in Table 8, the pressure residuals are smallest with the Wilson model as shown in Figure 17. The most significant error source in the measurement is the uncertainty on the density correlation according to the error analysis. Therefore, the densities of components should be determined in a reliable manner experimentally prior to VLE experiments for all pure components.

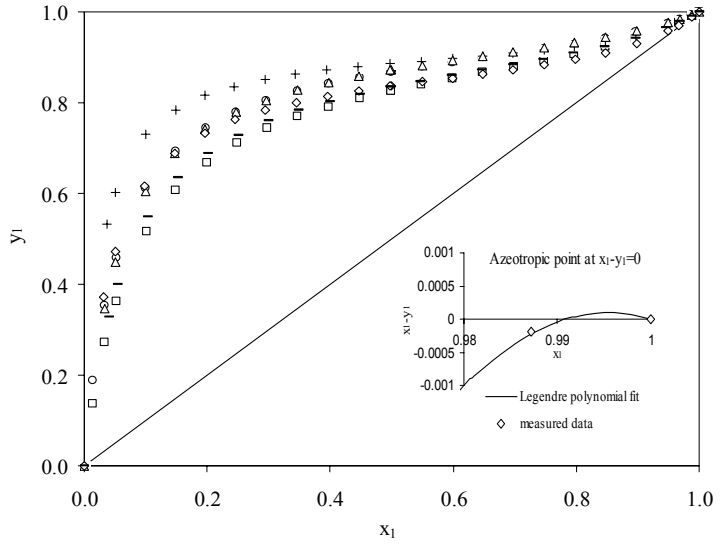

Figure 16. Composition diagram of *n*-butane (1) + 2-propanone (2) at 330.2 K: (◇), 2-methyl-propane (1) + 2-propanone (2) at 318.6 K: (+), 1-butene (1) + 2-propanone (2) at 323.3 K: (○), *cis*-2-butene (1) + 2-propanone (2) at 331.9 K: (□), 2-methyl-propene (1) + 2-propanone (2) at 323.1 K: (△), and *trans*-2-butene (1) + 2-propanone (2) at 332.1 K: (-).

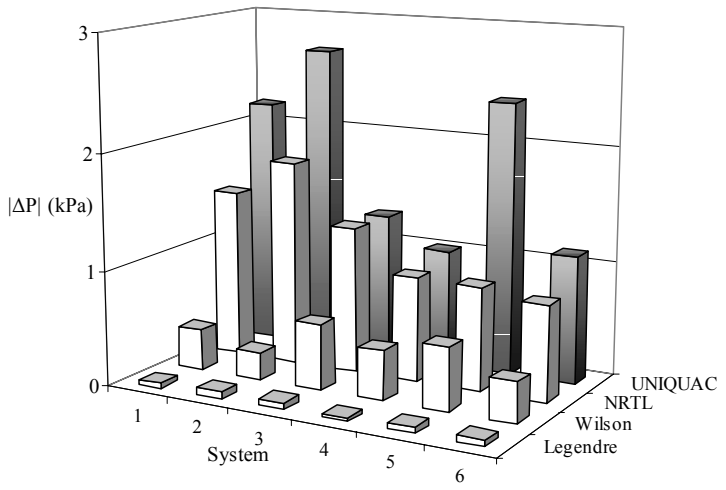

Figure 17. Absolute average pressure residuals between measured and calculated pressure about *n*-butane + 2-propanone (1), 2-methyl-propane + 2-propanone (2), 1-butene + 2-propanone (3), *cis*-2-butene + 2-propanone (4), 2-methyl-propene + 2-propanone (5), and *trans*-2-butene + 2-propanone (6).

Table 8. Parameters of activity coefficient models (Legendre, NRTL, Wilson and UNIQAC) and absolute average pressure residual $|\Delta P|$, liquid molar volume v_i, UNIQUAC volume parameter R_{UNIQ}, UNIQUAC area parameter Q_{UNIQ})

1 component	***n*-butane**	**2-methyl-propane**	**1-butene**	***cis*-2-butene**	**2-methyl-propene**	***trans*-2-butene**
2 component			**2-propanone**			
Legendre, $a_{1,0}$	1.423399	1.526581	1.0909	1.0253	1.027327	1.423399
Legendre, $a_{2,0}$	0.1172999	0.1279181	0.149740	0.15628	0.1506173	0.1172999
Legendre, $a_{3,0}$	0.070249	0.080643	0.054317	0.050452	0.044872	0.070249
Legendre, $a_{4,0}$	0.0129717	0.014963	0.012183	0.011517	0.0108872	0.0129717
Legendre, $a_{5,0}$	0.002732	0.003172	0.003835	0.003337	0.002924	0.002732
$\|\Delta P\|$ (kPa)	0.04	0.06	0.06	0.03	0.05	0.05
NRTL, λ_{12} (K)	338.5049	352.4253	301.6947	316.8406	308.6400	324.9956
NRTL, λ_{21} (K)	219.6852	234.5712	106.1589	80.0985	77.8910	89.8317
NRTL, $\alpha_{12} = \alpha_{21}$	0.4	0.4	0.4	0.4	0.4	0.4
$\|\Delta P\|$ (kPa)	1.46	1.78	1.27	0.91	0.90	0.83
Wilson, λ_{12} (J/mol)	1181.1	1310.1	434.3	307.6	253.6	366.4
Wilson, λ_{21} (J/mol)	3765.3	3933.8	3126.2	3146.6	3104.1	3237.6
v_i (cm^3/mol)	96.553	97.704	89.621	87.450	89.424	89.415
$\|\Delta P\|$ (kPa)	0.36	0.24	0.57	0.43	0.55	0.35
UNIQUAC, λ_{12} (K)	213.61	213.99	198.91	207.43	207.82	203.61
UNIQUAC, λ_{21} (K)	1.610	8.480	27.746	-38.926	6.378	-30.892
R_{UNIQ}	3.151	3.150	2.921	2.919	2.920	2.919
Q_{UNIQ}	2.776	2.772	2.564	2.563	2.684	2.563
$\|\Delta P\|$ (kPa)	2.17	2.69	1.26	1.01	2.36	1.10

6 Conclusion

Considering the fact that efforts to develop new oxygenate processes and to find alternatives to replace MTBE are developing, accurate vapor liquid equilibrium (VLE) data is essential for the new design of the separation units and a large number of other applications of industrial interest. In this work, either isobaric or isothermal VLE data and excess molar enthalpy measurements were carried out for the binary systems of 2,4,4-trimethyl-1-pentene with alcohols (2-propanol, ethanol, 2-butanol, and 2-methyl-2-propanol) as well as for the binary systems of 2,3-dimethyl-2-butene with alcohols (2-propanol, ethanol, 2-butanol, and methanol) at isobaric VLE system (atmospheric pressure). In the static total pressure apparatus, isothermal VLE data for C4-hydrocarbons with 2-propanone were measured. As 2-ethoxy-2-methylpropane (ETBE) has emerged as an alternative to MTBE, isobaric (atmospheric pressure) VLE data for a binary system of ETBE with components such as 2-propanol, 2-propanone and ethyl ethanoate as well as 1,1-diethoxyethane with these components were measured.

In addition, the experimental data were correlated using activity coefficient models and were also compared with a predictive activity coefficient model. The estimations made with different predictive coefficient models gave a worse description of the data when compared to that given by fitting the data with the Wilson equation. The experimental apparatus and the procedure presented here were shown to be reliable and particularly developed from the manually version to a computer-controlled of static apparatus. Moreover, our results are accurate, as they passed thermodynamic consistency tests. Most of the VLE and excess enthalpy in this thesis are for binary systems that have not been measured previously. The experimental apparatus built in this work is of great value since it allows the investigation of different binary systems as well as high-pressure VLE measurements.

REFERENCES

1. Fredenslund, Aa.; Gmehling, J.; Rasmussen, P. Vapor-liquid equilibria using UNIFAC-A group contribution method; Elsevier: Amsterdam, 1977.

2. Gmehling, J.; Lohmann, J.; Jakob, A.; Li, J.; Joh, R. A Modified UNIFAC (Dortmund) Model. 3. Revision and Extension. *Ind. Eng. Chem. Res.* **1998**, *37*, 4876-4882.

3. Kojima, K.; Tochigi, K. *Prediction of vapour-liquid equilibria by the ASOG method*; Kodanshia: Tokyo, 1970.

4. CRS repot for congress. *MTBE in Gasoline : Clean Air and Drinking Water Issues*, 98-290 ENR; 2003.

5. California Energy Commision. *Commission Findings: Timetable for the Phaseout of MTBE from California's Gasoline Supply*, DocKet NO. 99-GEO-1; 1999.

6. Yerazunis, S.; Plowright, J., D.; Smola, F., M. Vapor-Liquid Equilibrium Determination by a New Apparatus. *AIChE J.* **1964**, *10*, 660-665.

7. Poling, B. E.; Prausnitz, J. M.; O'Connell, J. P. The Properties of Gases and Liquid, 5th ed.; McGraw-Hill: New York, 2001.

8. David Raal, J.; Mühlbauer, A. L. Phase Equilibria Measurement and Computation, Taylor & Francis: America,1998.

9. Wilson, G., M. Vapor-liquid equilibrium XI: A new expression for the excess free energy of mixing. *J. Am. Chem. Soc*. **1964**, *86*, 127-130.

10. Renon,H.; Prausnitz, J.M. Local compositions in thermodynamic excess functions for liquid mixtures. *AIChE J*, **1968**, *14*, 135-144.

11. Abrams, D. S.; Prausnitz, J. M. Statistical Thermodynamics of Liquid Mixtures: A new Expression for the Excess Gibbs Energy of Partly or Completely Miscible System, *AIChE J.* **1975**, *21*, 116-128.

12. Gmehling, J.; Onken, U. Vapour-liquid equilibrium data collection, DECHEMA chemistry data series; Vol 1, part 1, DECHEMA: Frankfurt/Main, 1977.

13. Wisniak. J. The Herington Test for Thermodynamic Consistency. *Ind. Eng. Chem. Res.* **1994**, *33*, 177-180.

14. Van Ness, H. C. Classical Thermodynamics of Non-Electrolyte Solutions, Pergamon Press, Oxford,1964.

15. Redlich, O.; Kister, A. T. Algebraic Representation of Thermodynamic Properties and the Classification of Solutions. *Ind. Eng. Chem*. **1948**, *40*, 345-348.

16. Herinton, E. F. G. Tests for the Consistency of Experimental Isobaric Vapour-liquid Equilibrium Data. *J. Inst. Pet*. **1951**, *37*, 457-470.

17. Kojima, K.; Moon, H.; Ochi, K. Thermodynamic Consistency Test of Vapor-Liquid equilibrium Data. *Fluid Phase Equilib*. **1990**, *56*, 269-284.

18. Fenclová, D.; Vrbka, P.; Dohnal, V.; Řehák, K.; Miaja, G. G. (Vapour + liquid) equilibria and excess molar enthalpies for mixtures with strong complex formation. Trichloromethane or 1-bromo-1-chloro-2,2,2-trifluoroethane (halothane) with tetrahydropyran or piperidine. *J. Chem. Thermodyn*. **2002**, *34*, 361-376.

19. Pokki, J.-P.; Laakkonen, M.; Uusi-Kyyny, P.; Aittamaa, J. Vapor-liquid equilibrium for the *cis*-2-butene + methanol, + ethanol, + 2-propanol, + butanol and + 2-methyl-2-propanol systems at 337 K. *Fluid Phase Equilib*. **2003**, *212*, 129-141.

20. Laakkonen, M.; Pokki, J.-P.; Uusi-Kyyny, P.; Aittamaa, J. Vapor –liquid equilibrium for the 1-butene + methanol, + ethanol, + 2-propanol, + 2-butanol and + 2-methyl-2-propanol systems at 326. *Fluid Phase Equilib*. **2003**, *206,* 237-252.

21. Uusi-Kyyny, P.; Pokki, J.-P.; Laakkonen, M.; Aittamaa, J.; Liukkonen, S. Vapor liquid equilibrium for the binary systems 2-methylpentane + 2-butanol at 329.2 K and *n*-hexane + 2-butanol at 329.2 and 363.2 K with a static apparatus. *Fluid Phase Equilib*. **2002**, *201* 343-358.

22. Thomson, G. H.; Brobst, K. R.; Hankinson, R. W. An improved correlation for densities of compressed liquids and liquid mixtures. *AIChE J*. **1982**, *28*, 671-676.

23. Barker, J. A. Determination of Activity Coefficient from Total Pressure Measurements. *Aust. J. Chem*. **1953**, *6*, 207-210.

24. J. Aittamaa, J.-P. Pokki, User manual of program VLEFIT, Helsinki University of Technology, Espoo, 2003.

25. Van Ness, H. C. Abbott, M. M. Classical Thermodynamics of Nonelectrolyte Solutions, McGraw-Hill, New York, 1982.

26. Mani, J.-C.; Cuony, B. Measurement of Vapour/liquid Equilibria with an Automatic Lab Reactor, METTLER TOLEDO publication 51724657.

27. Lozano, L. M.; Montero, E. A.; Martine, M.C.; Villamanan, M.A. Vapor –liquid equilibria of binary mixtures containing methyl tert-butyl ether (MTBE) and/or substitution hydrocarbons at 298.15 K and 313.15 K. *Fluid Phase Equilib*. **1995**, *110*, 219-230.

28. Soave, G. Equilibrium constants from a modified Redlich-Kwong equation of state. *Chem. Eng. Sci*. **1972**, *27*, 1197-1203.

29. Daubert, T. E.; Danner, R. P. Physical and Thermodynamic Properties of Pure Chemicals: Data Composition, Hemispere, New York, 1989.

30. Abrams, D. S.; Prausnitz, J. M. Statistical Thermodynamics of Liquid Mixtures: A new Expression for the Excess Gibbs Energy of Partly or Completely Miscible System, *AIChE J.* **1975**, *21*, 116-128.

31. Krähenbühl, M.; Gmehling, J. Vapor Pressures of Methyl *tert*-Butyl Ether, Ethyl *tert*-Butyl Ether, Isopropyl *tert*-Butyl Ether, *tert*-Amyl Methyl Ether, and *tert*-Amyl Ethyl Ether. *J. Chem. Eng. Data* **1994**, *39*, 759-762.